Universidad Autónoma de Sinaloa

Facultad de Ciencias Físico-Matemáticas

"Performance of AD detector in Beam-Test"

M.C. Solangel Rojas Torres*
Dr. Ildefonso León Monzón*
Dr. Gerardo Herrera Corral**

* Universidad Autónoma de Sinaloa.
**Centro de Investigación y de Estudios Avanzados del Instituto Politécnco Nacional

4/11/2017

Content

- ALICE Diffractive detector.
- Beam test setup.
- Results and discussion.
  - Efficiency.
  - Border analysis.
  - Time and charge analysis.
- Final comments.

AD detector

- Study of diffractive physics is of a great interest topic for LHC CERN.
- ALICE have an excellent tracking and particle identification, providing a good capabilities to investigate diffractive production as can be seen in [2] [3] ,proving that is possible to measure single and double diffractive processes.
- ALICE Diffractive was designed to improve the sensitivity of ALICE increasing the pseudorapidity coverage of the experiment.

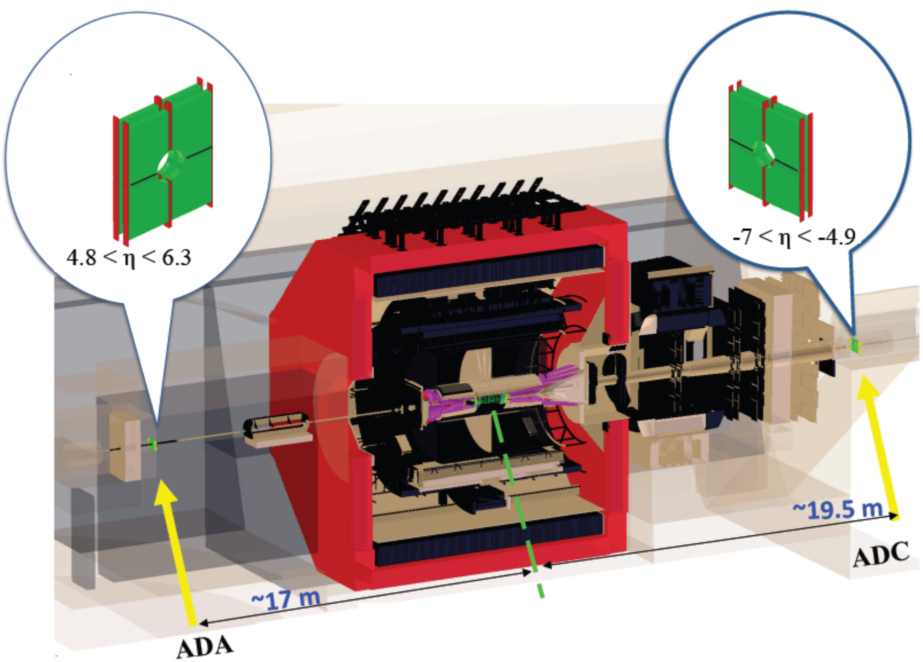

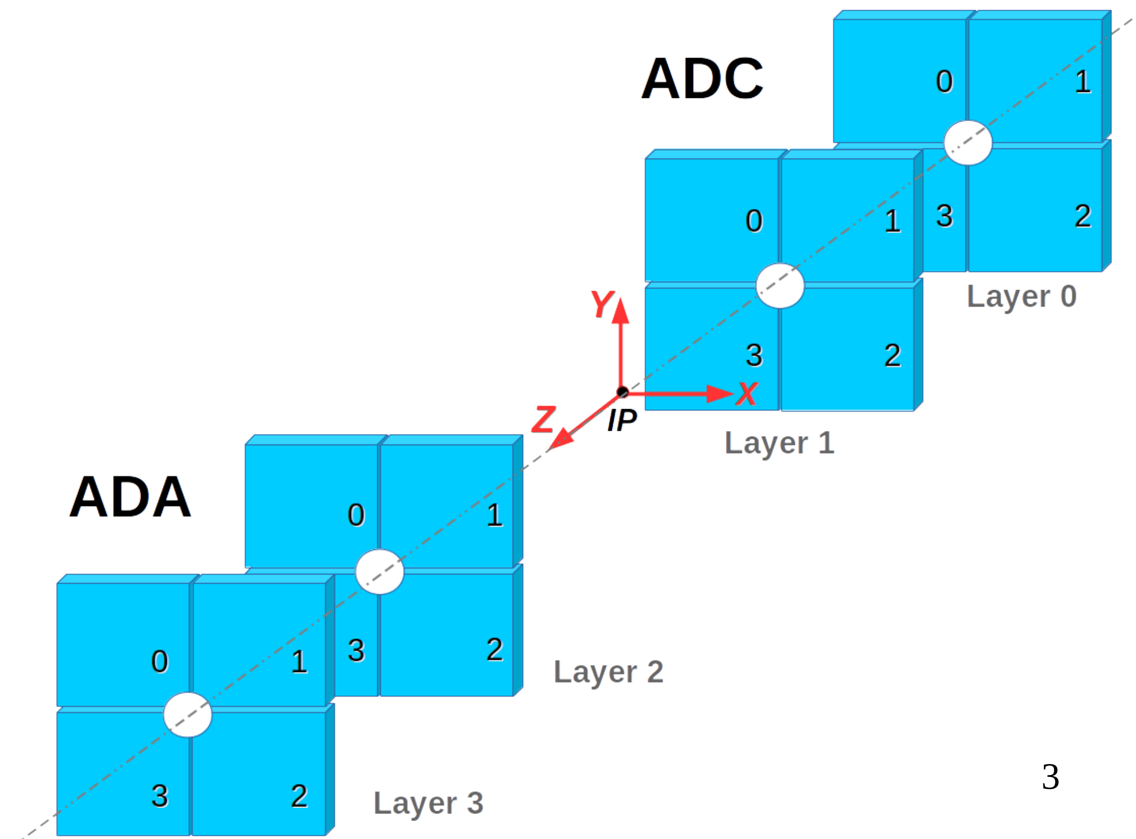

Mechanical design and geometry

- **Plastic scintillator: *BC-404***
- **WLS bars: *ELJEN (EJ-280)***
- **Optical fibers: *Kuraray (PSM-Clear)***
- **PMTs: *Hamamats- R5946 (16 dinodes)***

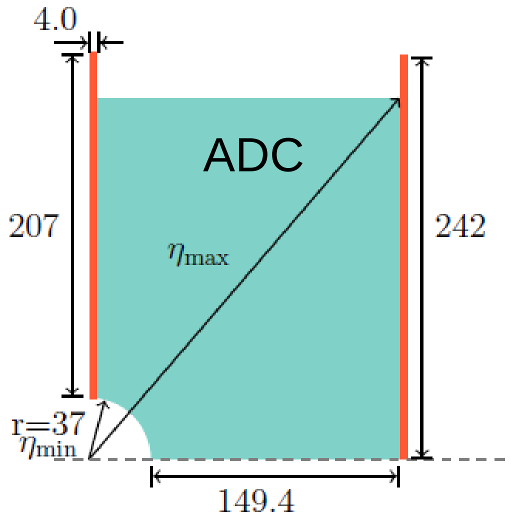

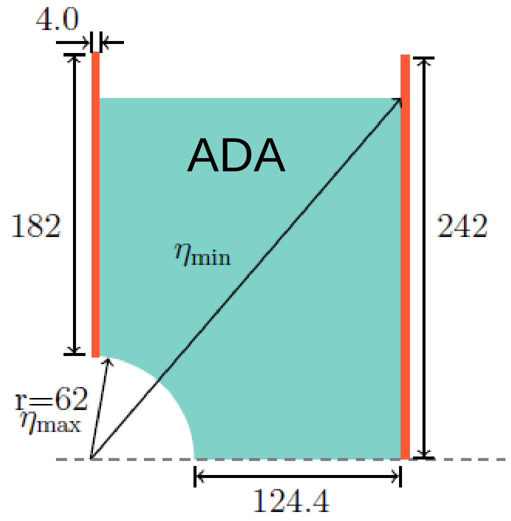

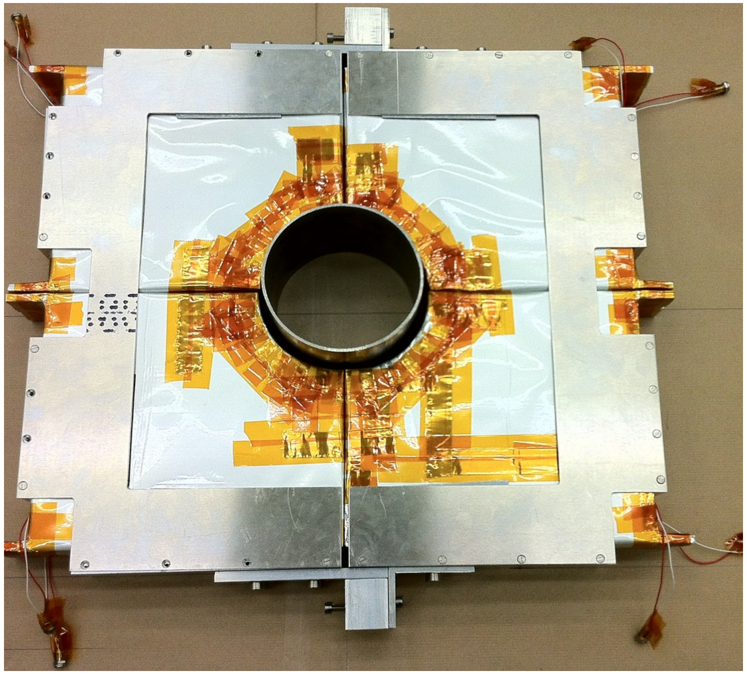

Beam-test Setup

- Were used two kind of detectors for trigger:
  1) Scintillator hodoscopes → **Black-Left** and **Black-Right**
  2) Cherenkov radiators → **T0-end** and **T0-start**

- In a special run were measured the properties of the WLS bar using a pixel detector at **1.5 GeV/c**.
- The momentum of the beam for the general scans was set at **1 GeV/c**, and some extra runs were taken at **1.5**, **2** and **6 GeV/c**.
- Were used an ADA and ADC modules, labeled as AD1 and AD2 respectively.

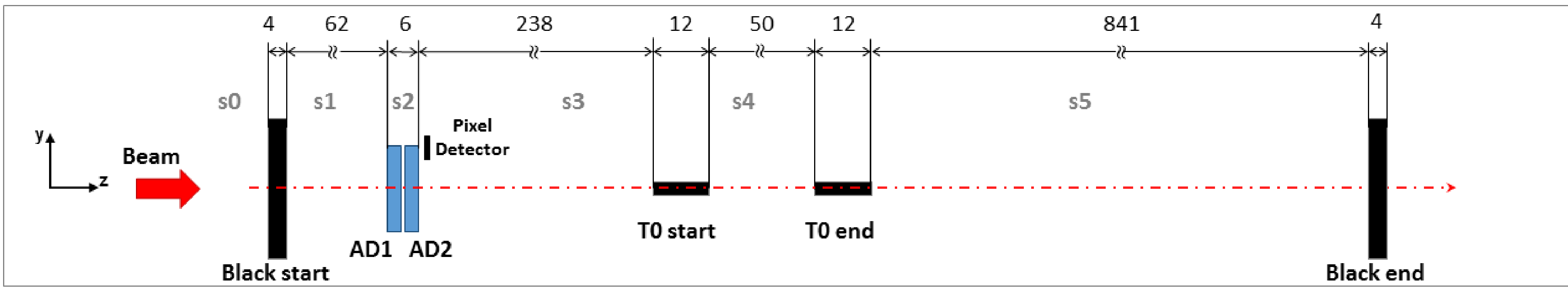

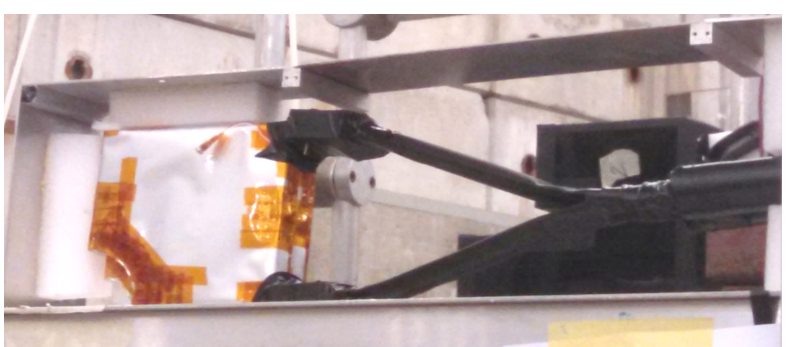

5

Front End Electronic integration

FEE system installed for the beam test. The same electronic system as the one installed in ALICE.

Configuration and connexions during the beam test.

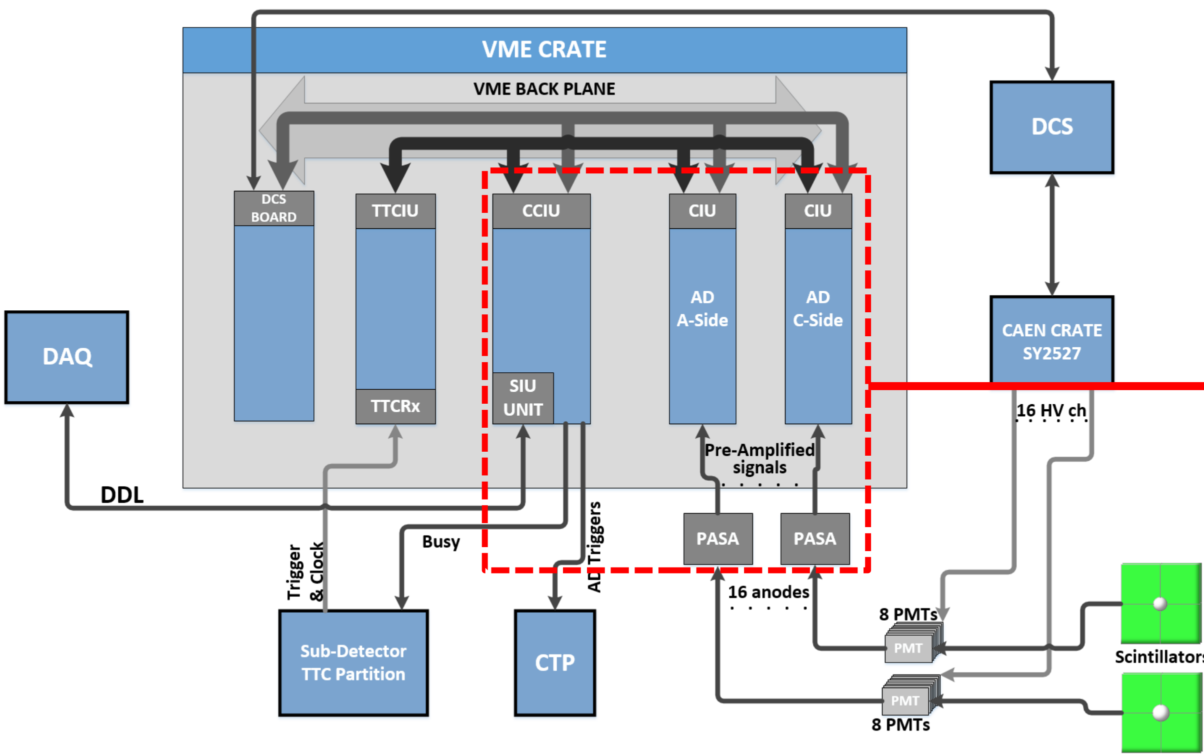

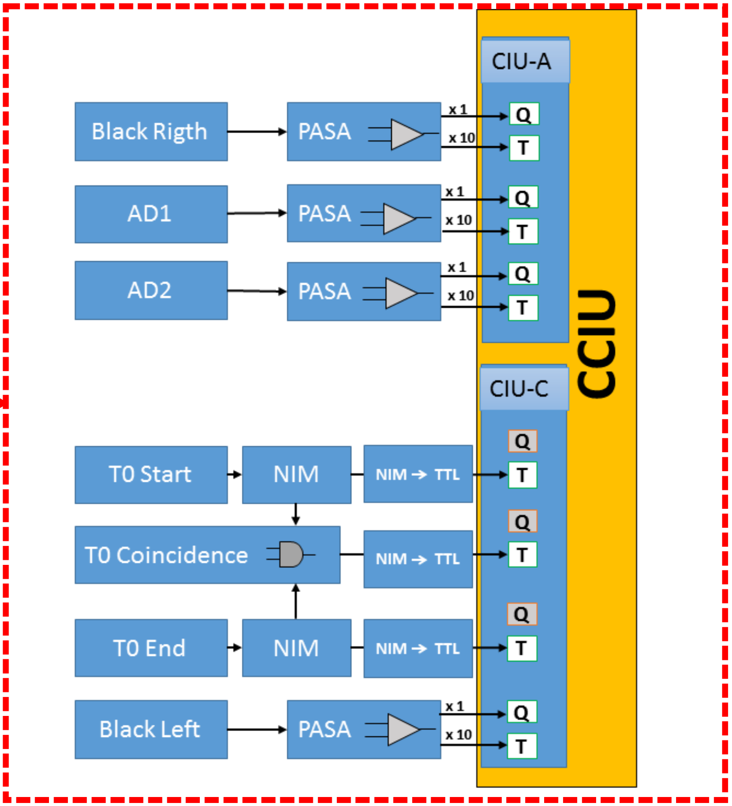

Beam-test Setup (table positions)

- In the table below can be seen:
  - ✓ The table positions.
  - ✓ T0 detector overlap area.
  - ✓ Collimator aperture.
  - ✓ Beam momentum.

- The fiber length used for the test was 47 cm.
- Were done scans along the Y and X axis respect to the points shown in the the draw shown at the right.

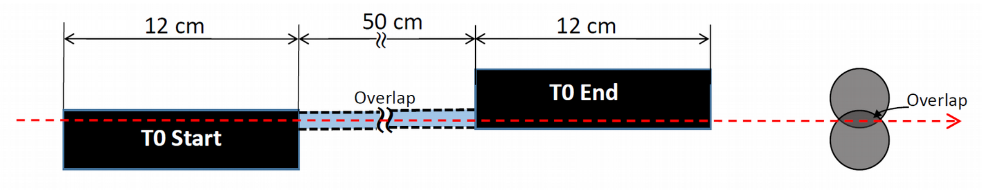

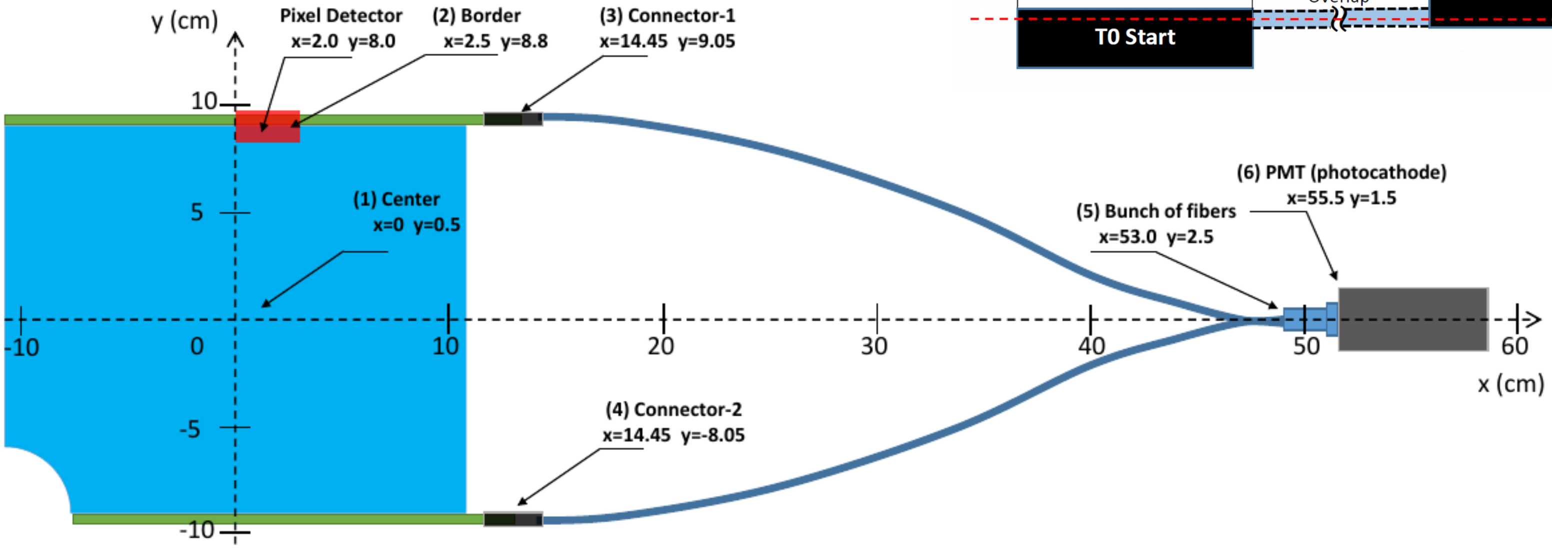

No.	Section	x position (cm)	y position (cm)	T0 overlap (cm)	Collimator (cm)	Entries
1	Center	0	0.5	0.2	2.4	18561
2	Border	2.5	8.8	0.1	4.0	250159
3	Conn. 1	14.45	9.05	0.1	2.4	1071
4	Conn. 2	14.45	-8.05	0.1	2.4	1020
5	Fiber	53.0	-1.5	0.1	2.4	47117
6	PMT	55.5	-0.5	0.1	2.4	2357
	WLS (pixel)	2.0	8.0	2.0	0.5	32640

Results and discussion

Efficiency and charge plots

Scan a long the center

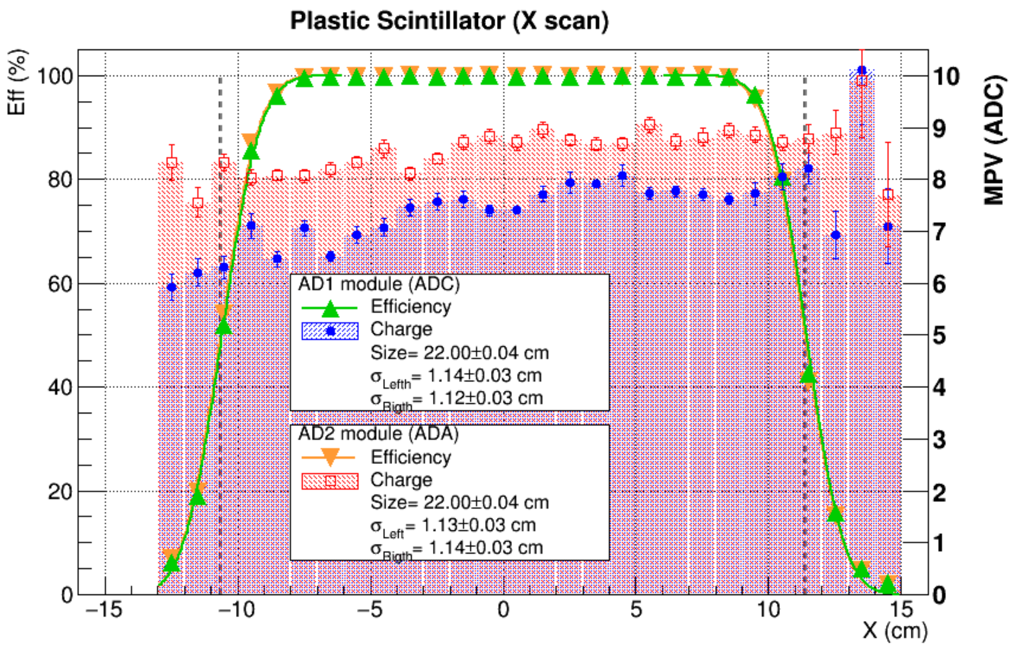

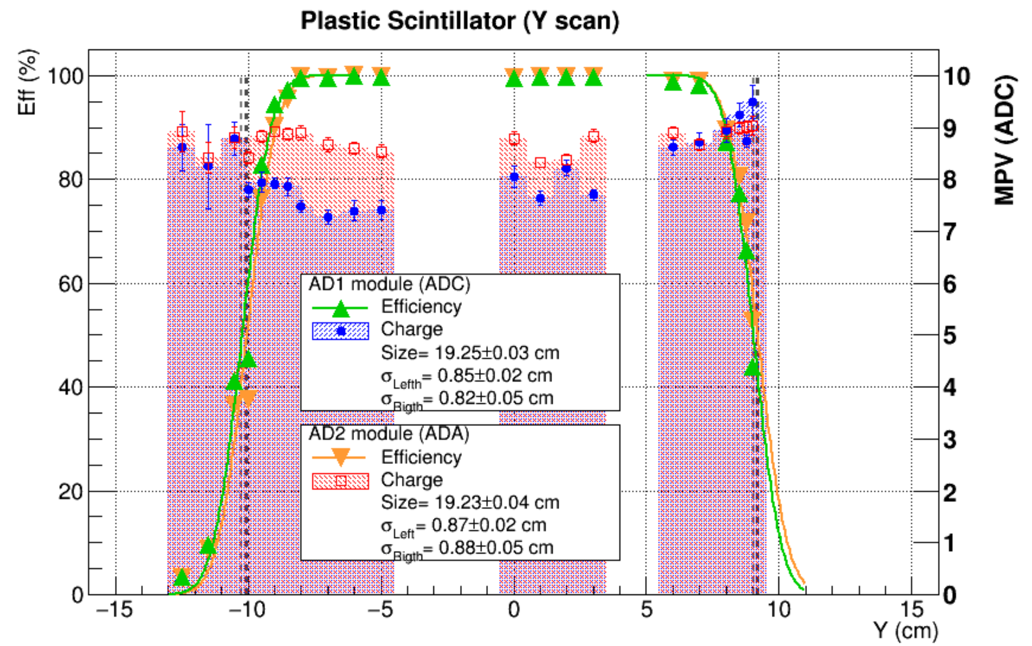

Efficiency calculation :

$$\text{Efficiency} = \frac{N}{N_{\text{total}}} = \frac{\text{T0-start} \wedge \text{T0-end} \wedge \text{AD}}{\text{T0-start} \wedge \text{T0-end}}$$

Was fitted a Cumulative gaussian distribution to the borders :

$$p = F(x|\mu,\sigma) = \frac{1}{\sigma\sqrt{2\pi}} \int_{-\infty}^{x} e^{\frac{-(t-\mu)^2}{2\sigma^2}} dt$$

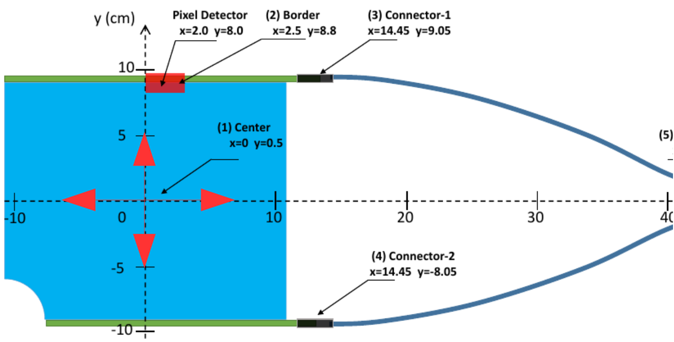

Charge calculation :

- Where selected Time≠0 events.
- Was fitted a Landau+Gaussian distribution and MPV value was taken

Efficiency and charge plots
Scan a long the center

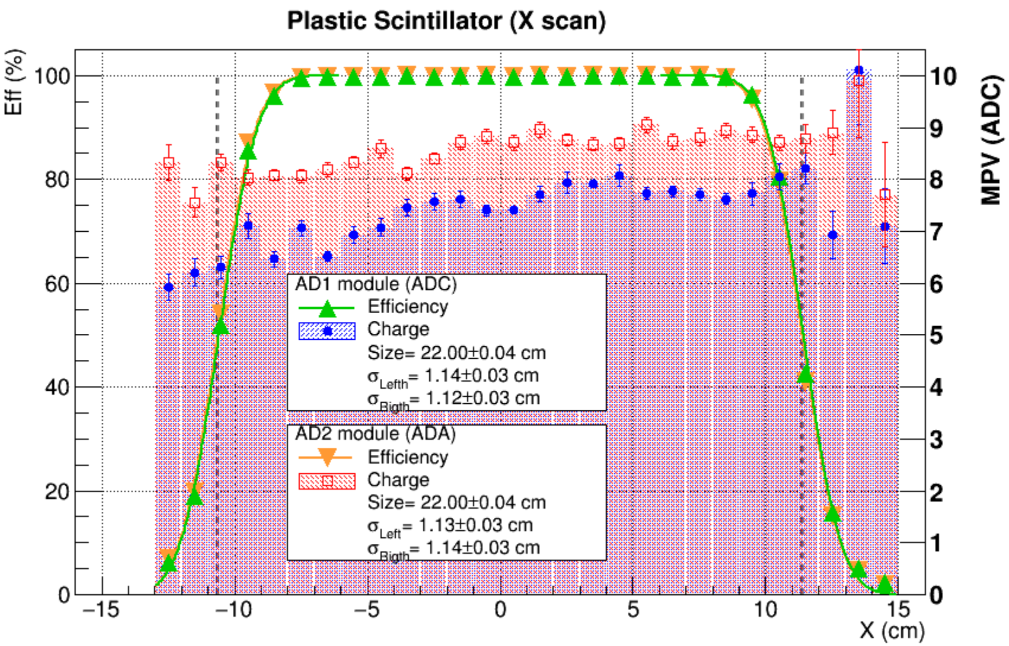

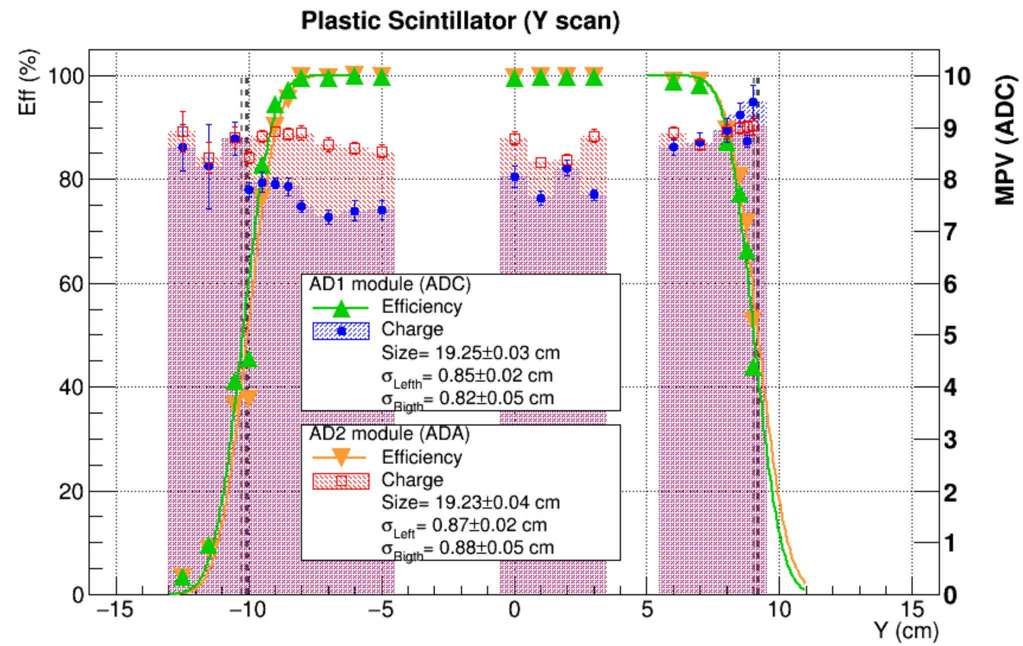

The mean of the borders of both modules allow us to estimate the size of the modules.

	X-axis length (*mm*)	Y-axis length (*mm*)
Real	216	181
AD1	220 ± 0.35	192.32 ± 0.4
AD2	219.9 ± 0.35	192.49 ± 0.32

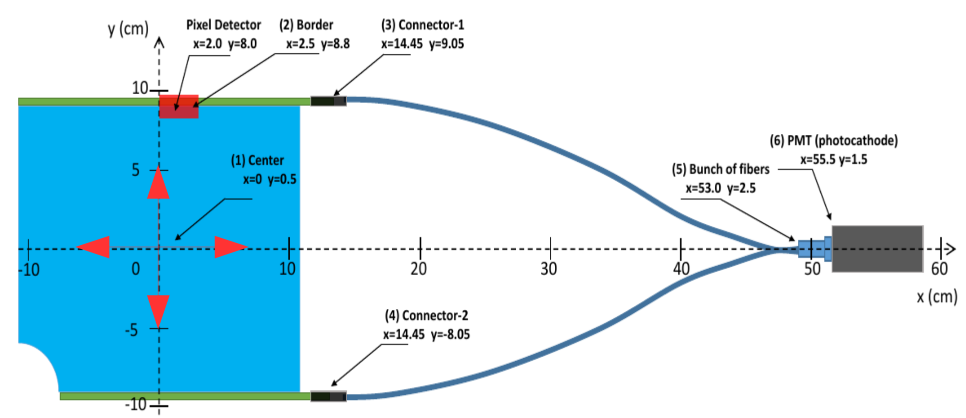

An estimation* of the beam size was calculated using the sigma information of the gaussian cumulative distribution function:

σ_x=11.29 ± 0.31 mm

σ_y=8.53 ± 0.16 mm

**Average of four sigma, two sides and modules per axis.*

Efficiency and charge plots
Scan a long Connectors

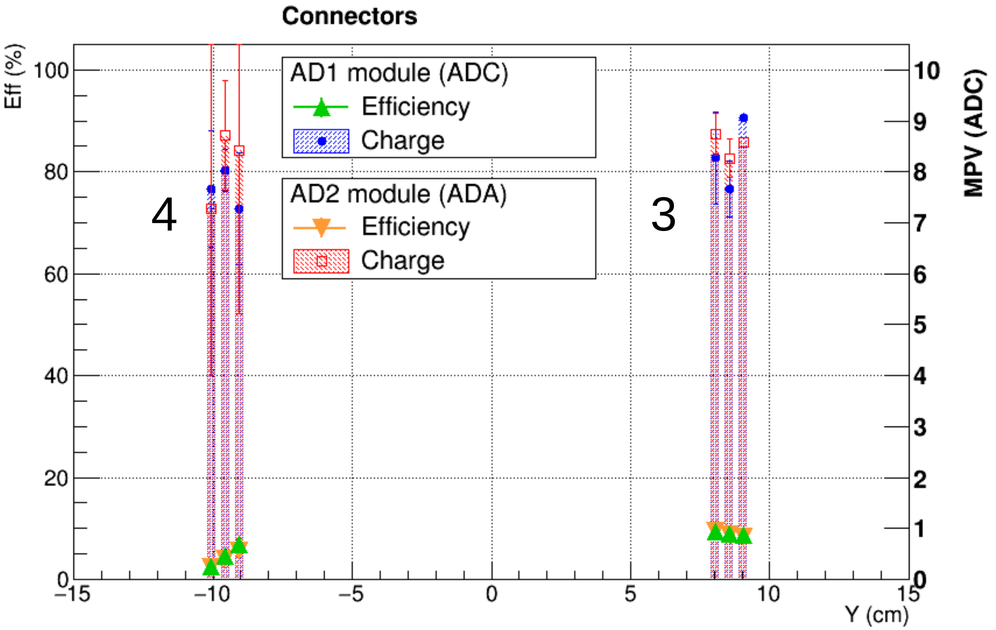

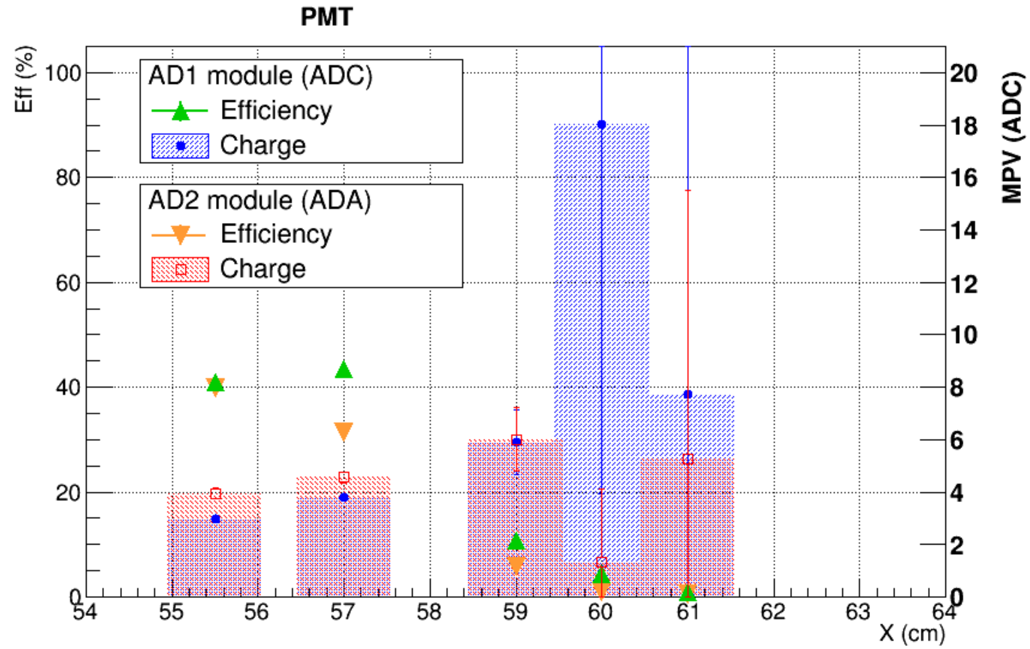

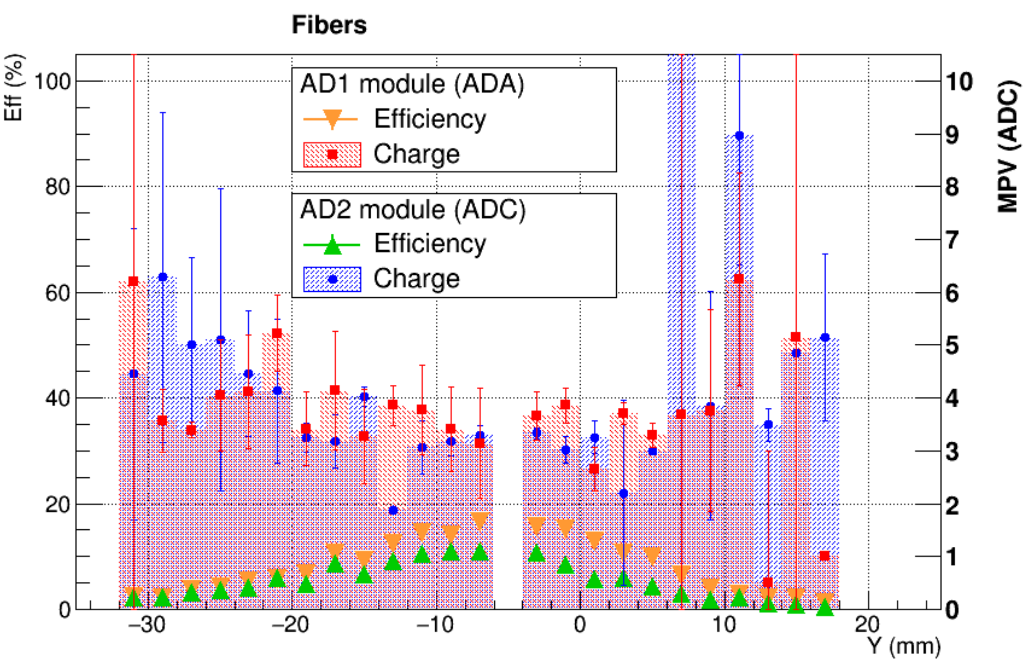

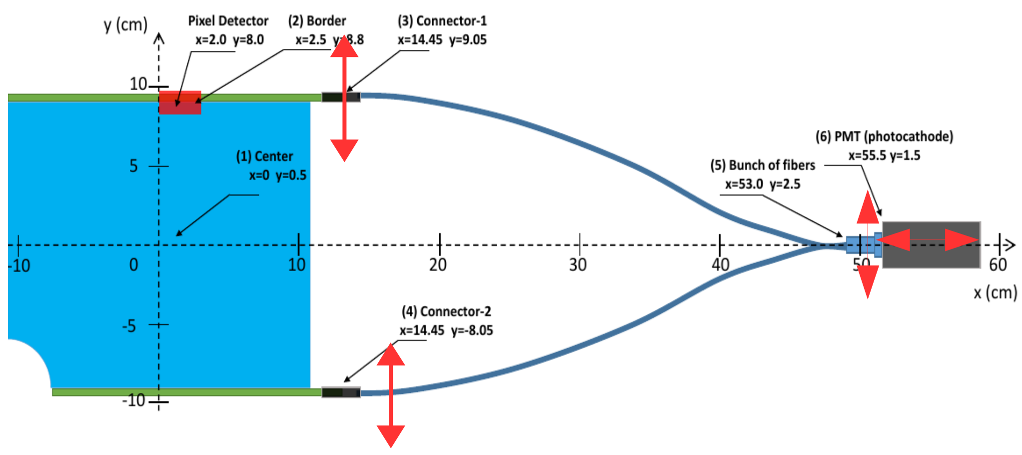

Border Analysis (Pixel detector)

Border analysis

The pixel detector* was placed behind the AD modules to get a precise information of the characteristics in the WLS bar.

Pixel Area:
1024 * 512 pixels
3 * 1.5 cm²

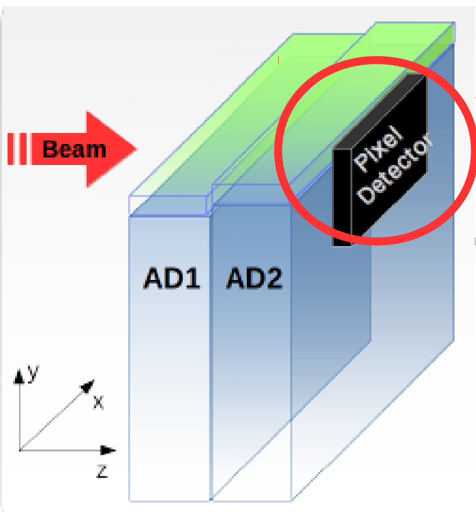

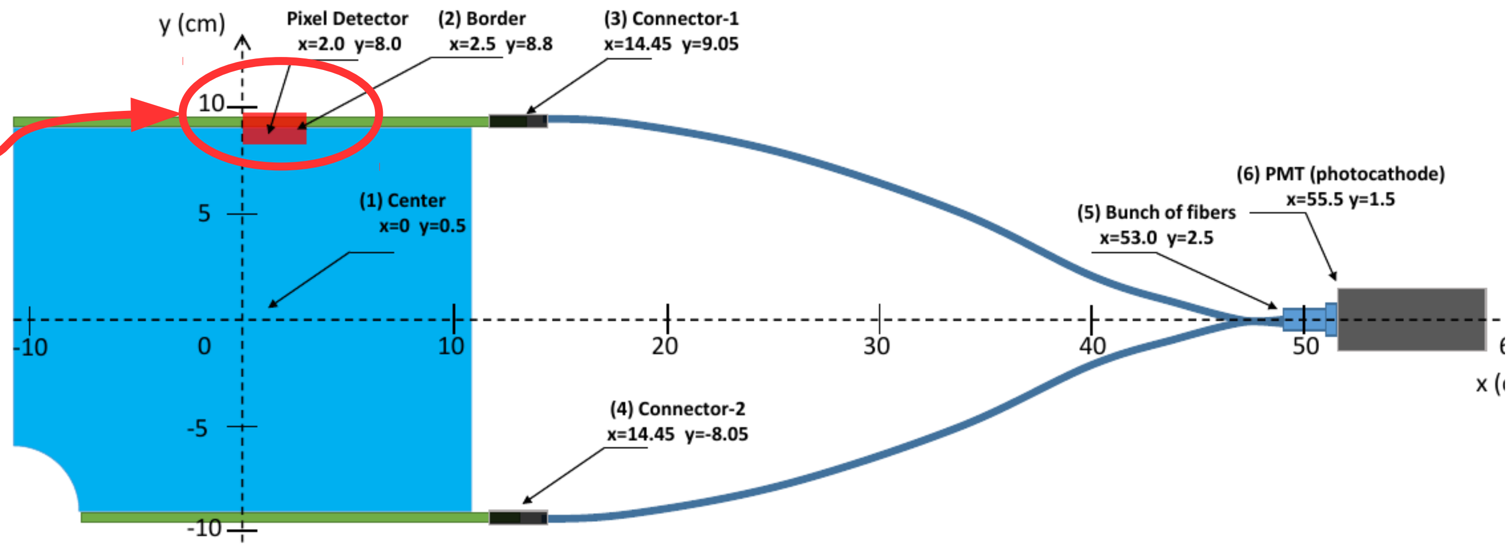

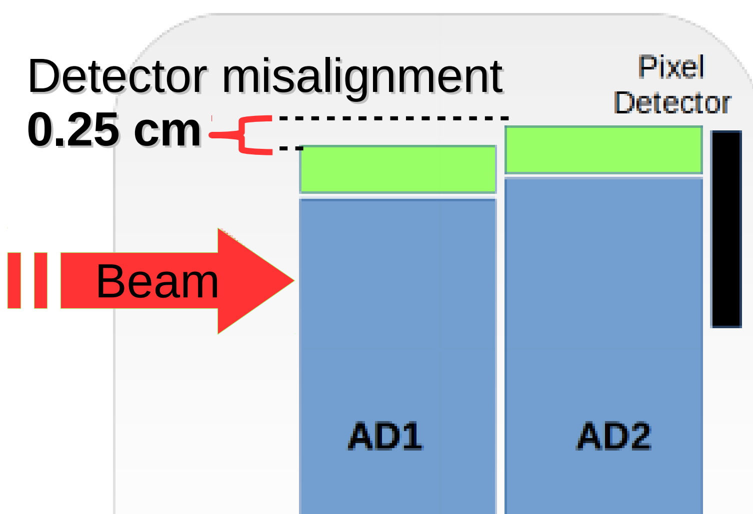

* Povided by ITS group (arxiv:1607.01171)

Charge and Time vs Pixel position

Hits distribution in pixel detector.

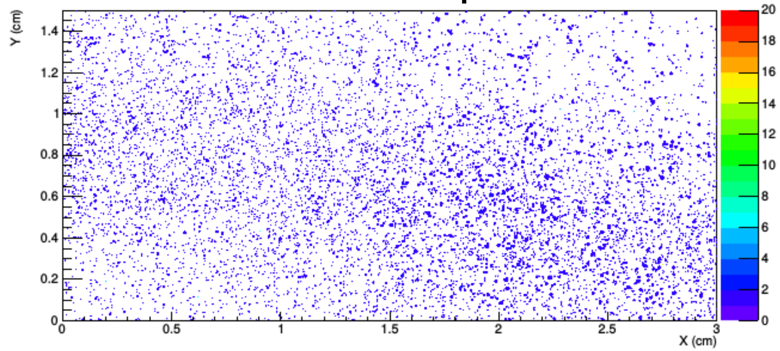

Top row:

- **Charge** and **time** respect to the horizontal pixel position (**X axis**).
- The responce is along this axis is **homogeneus**.

Bottom row:

- **Charge** and **time** respect to the vertical pixel position (**Y axis**).
- In this axis is seen the border effect.

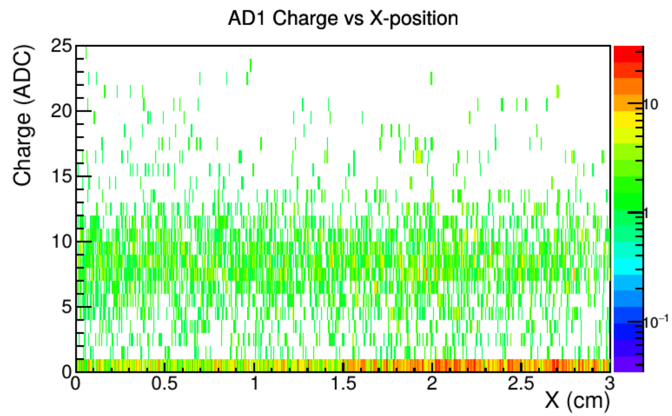

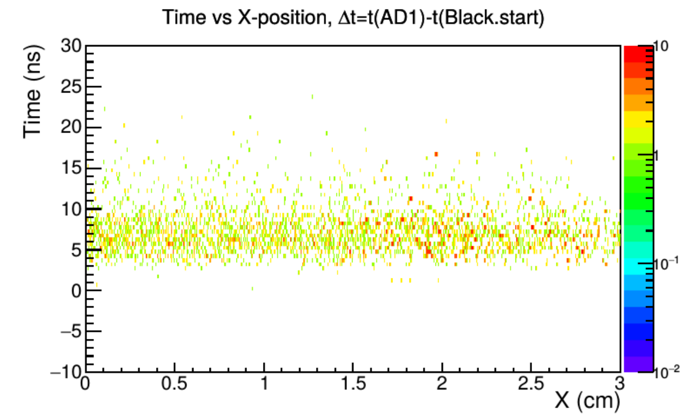

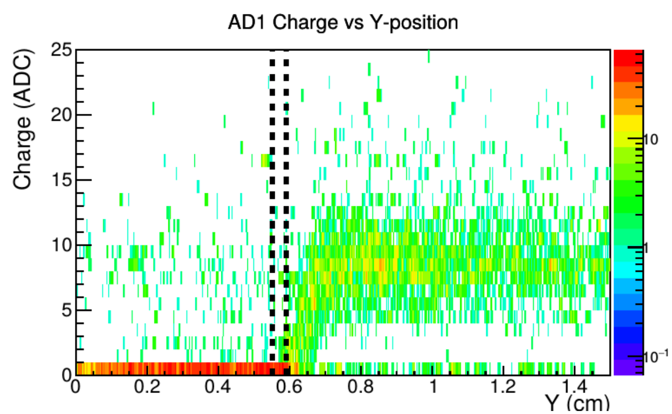

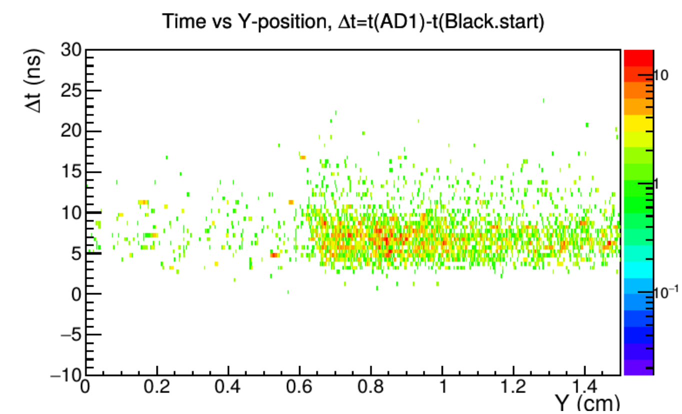

Regions definition for analysis

Charge vs Y pixel position*

Selection of event in WLS Bar and plastic scintillator

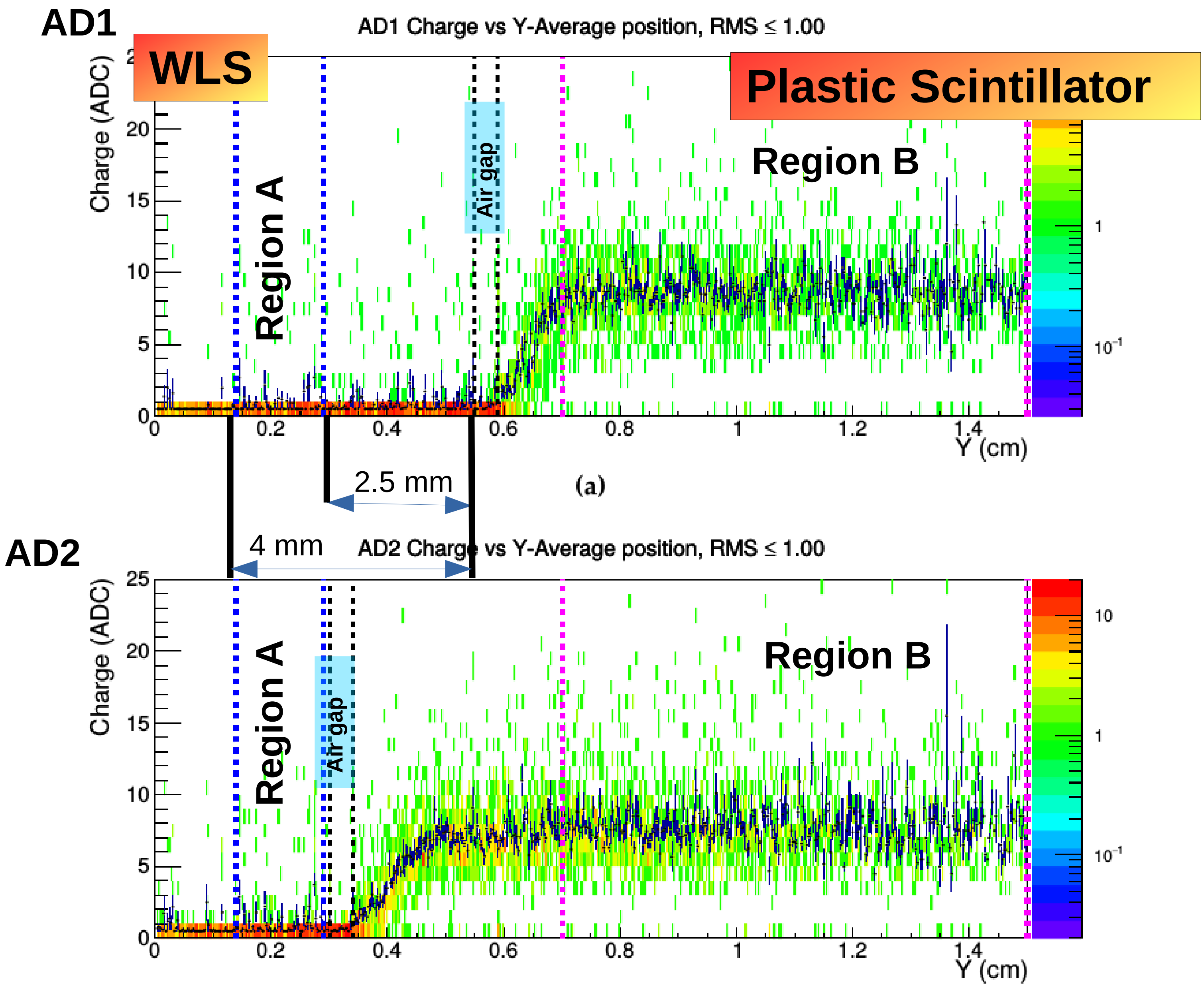

*Due that in a single event triggered can be fired several pixels, was used an average pixel position per event.

Number of pixel fired VS RMS (of pixels positions)

The RMS value of the pixels position fired on every event was calculated in order to clean the data.

Scintillator (Region B)

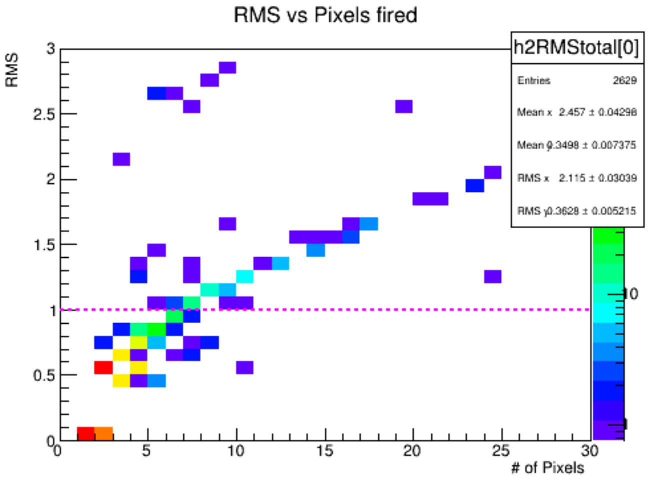

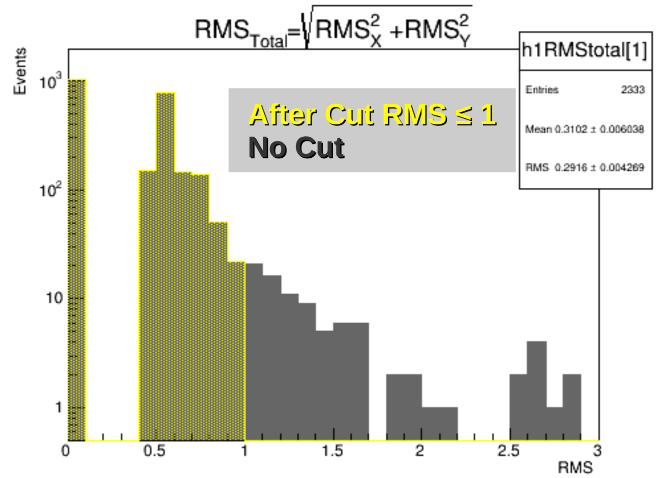

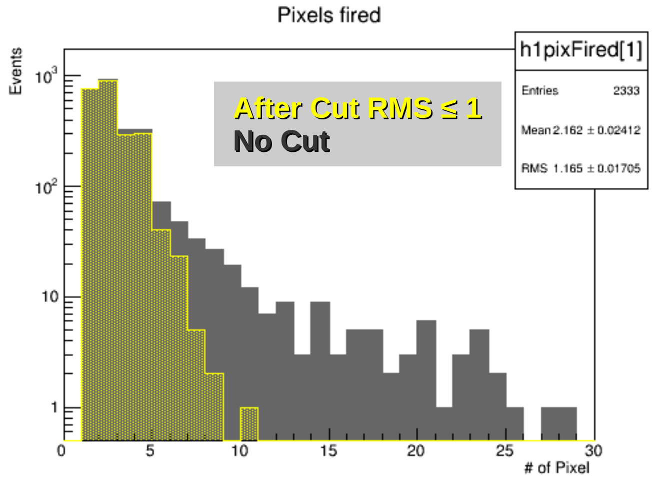

WLS (Region A)

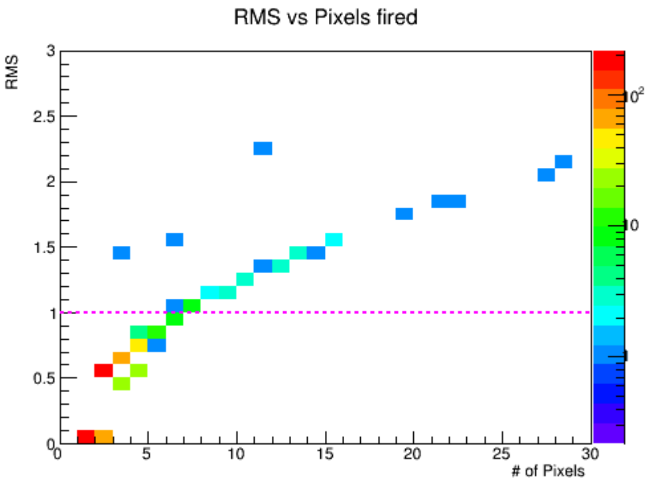

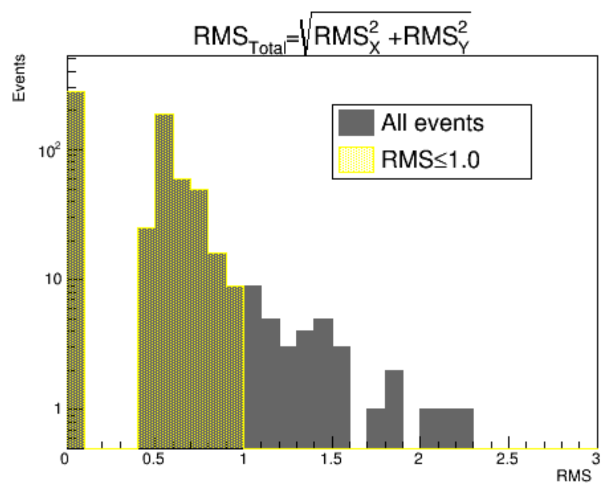

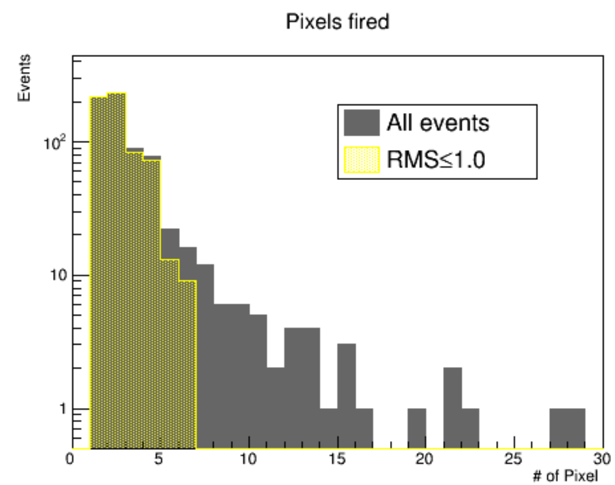

Same for AD1 and AD2

Charge correlation of AD1 vs AD2

Cut → RMS ≤ 1

Region A

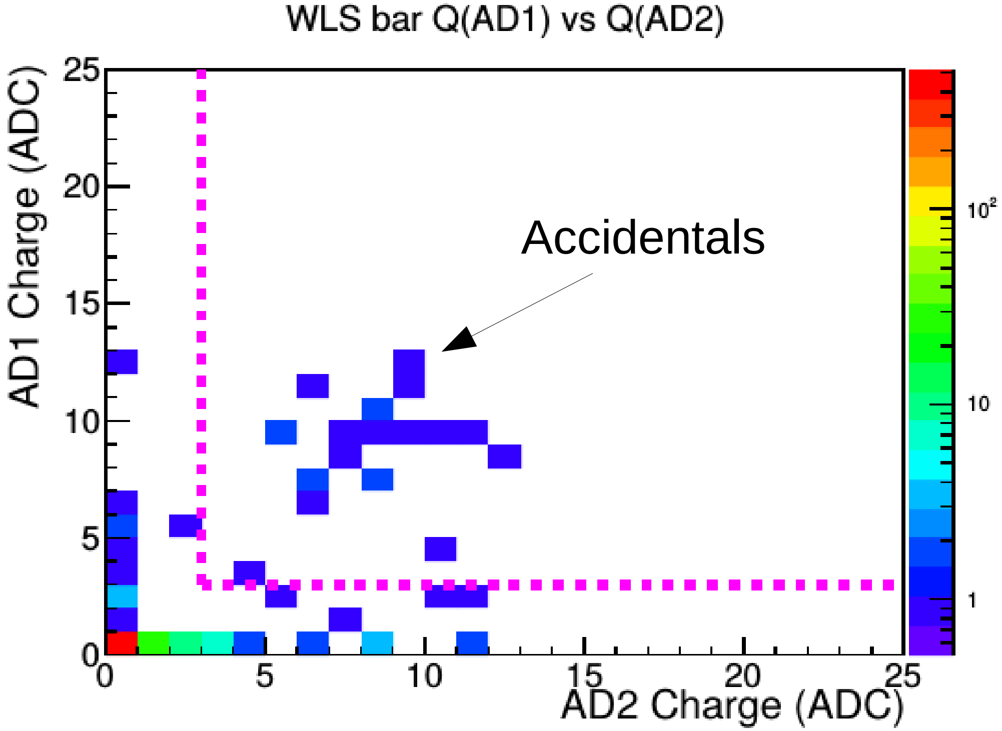

Region B

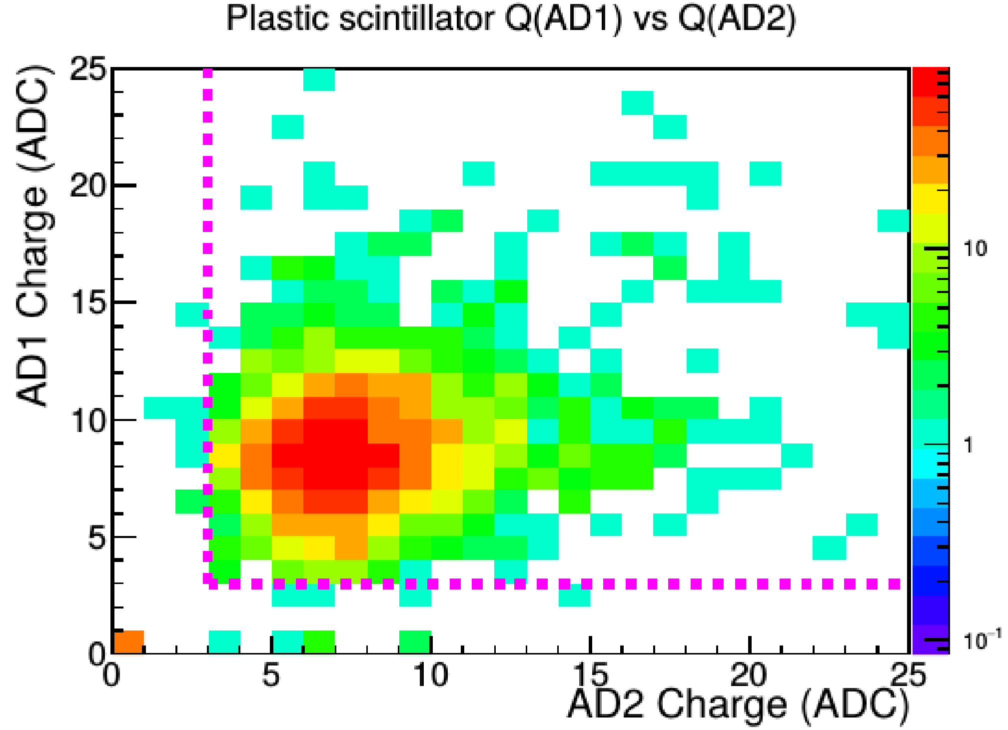

Charges selection events

Pixel position Average

Selection:
Q(AD1) $\leq$ **3** or **Q(AD2)** $\leq$ **3**

AD1

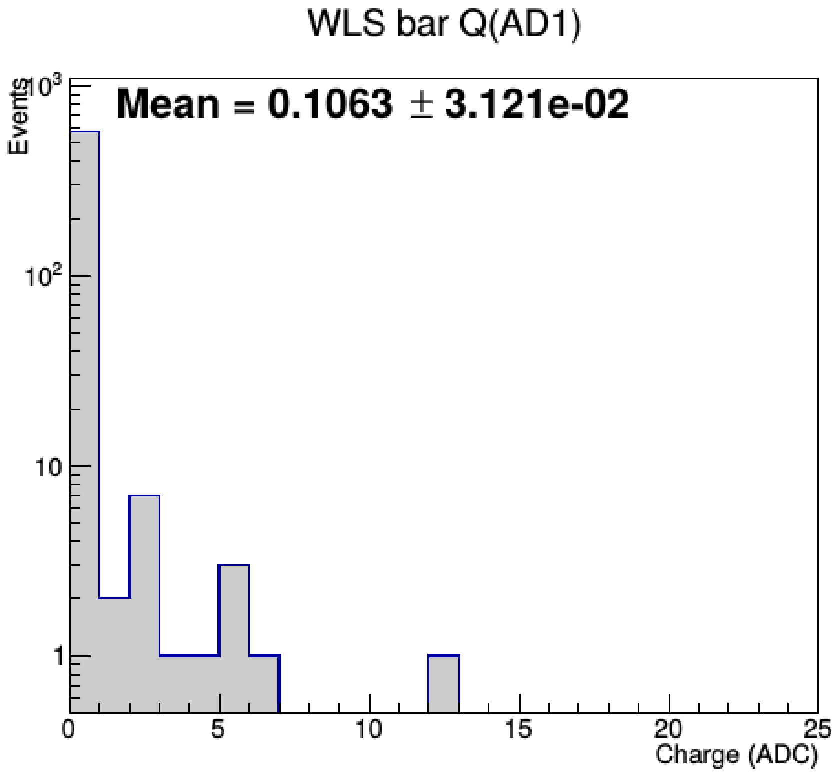

AD2

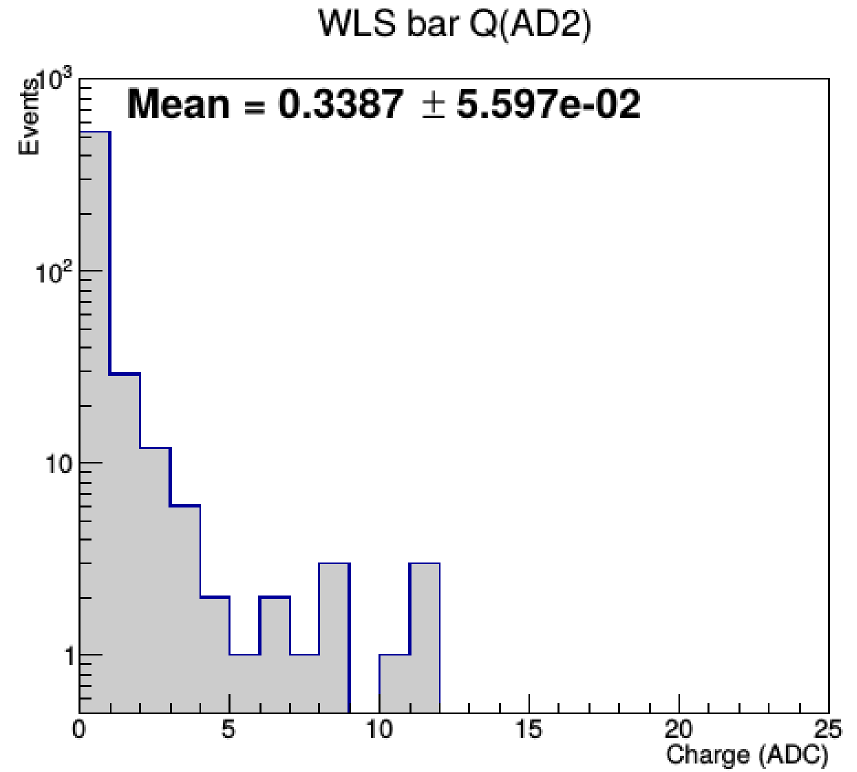

Results for the charge distribution after the selection.
The charge produced in the WLS bar is less than one ADC count, consistent with zero because the electronic system can not measure fractions of ADC (0.6 pC per ADC count).

WLS-bar efficiency analysis

$$\text{Eff.} = \frac{\text{Black-start} \wedge \text{Black-end} \wedge \text{Pixel} \wedge \text{AD}}{\text{Black-start} \wedge \text{Black-end} \wedge \text{Pixel}}$$

- Time flags used to calculate the efficiency.
- RMS cut was applied.

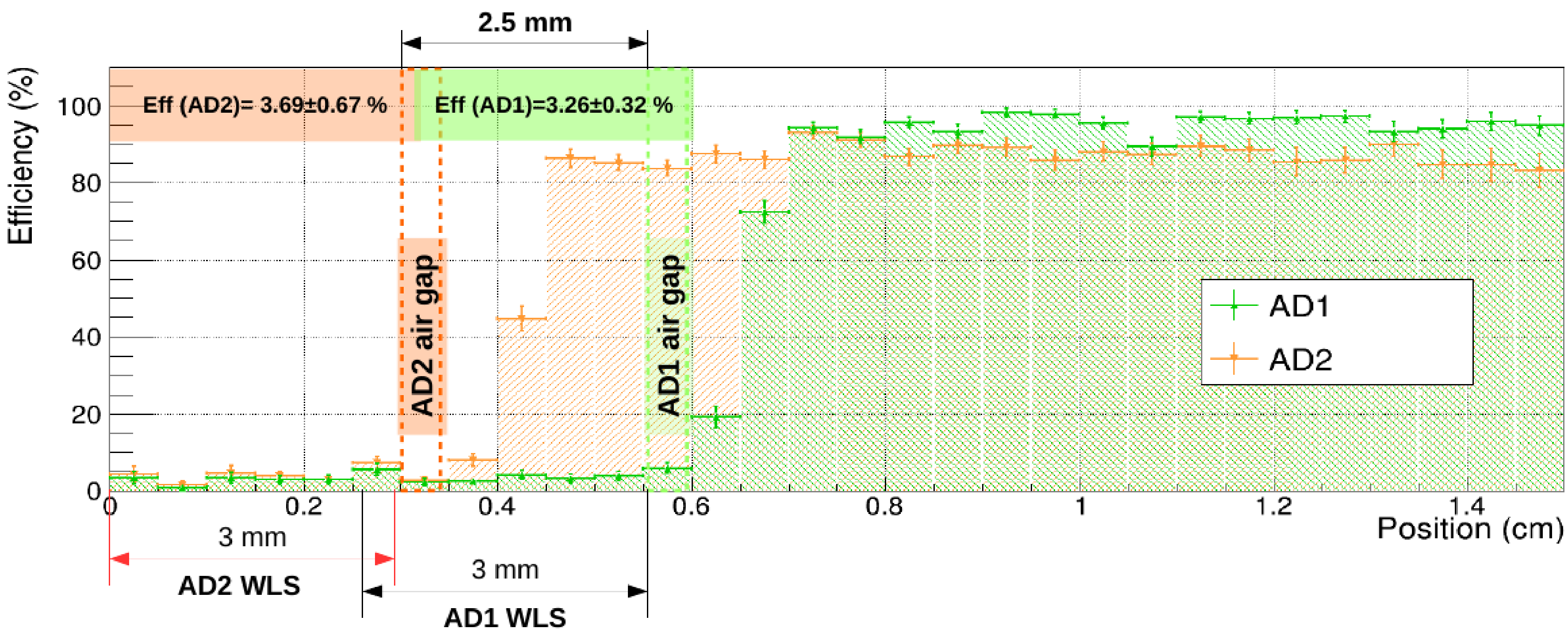

	WLS bar (%) (3 mm zone)
AD1	**3.688 ± 0.668**
AD2	**3.264 ± 0.317**

Time and Charge analysis

Time measurement

The particle selection was made using **Black-start** and **T0-end** time difference.

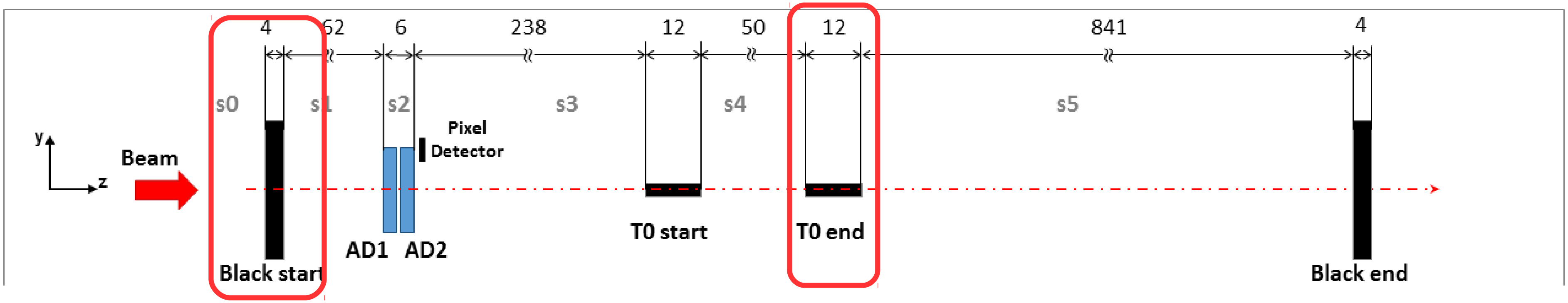

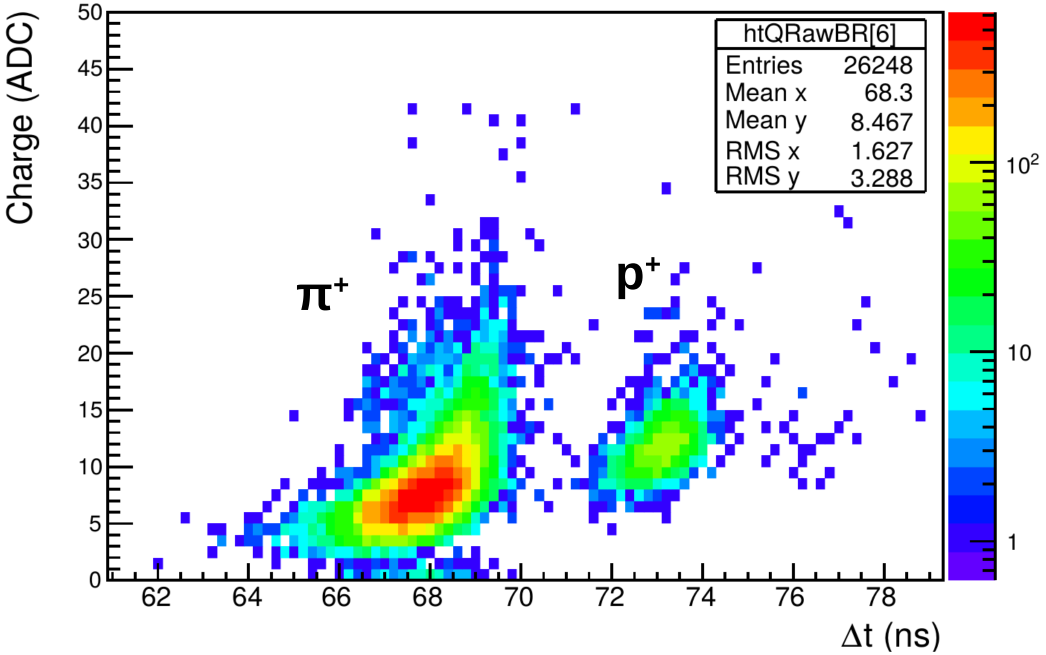

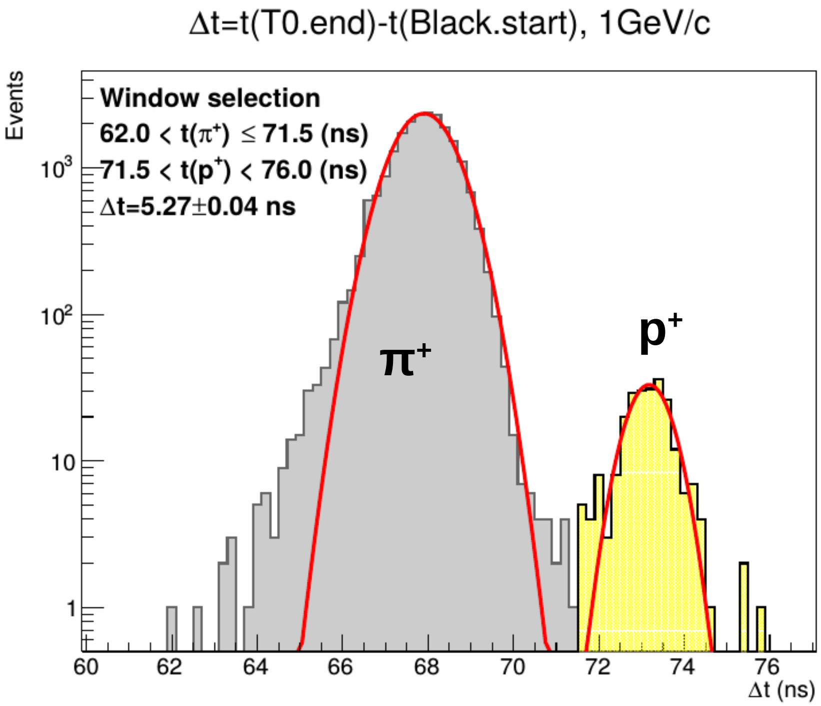

Time measurement

- The time response of the AD modules have been analyzed respect to T0-end detector.
- T0-end have a good time resolution of ~50 ps.
- The beam momentum was set at 1 GeV/c.

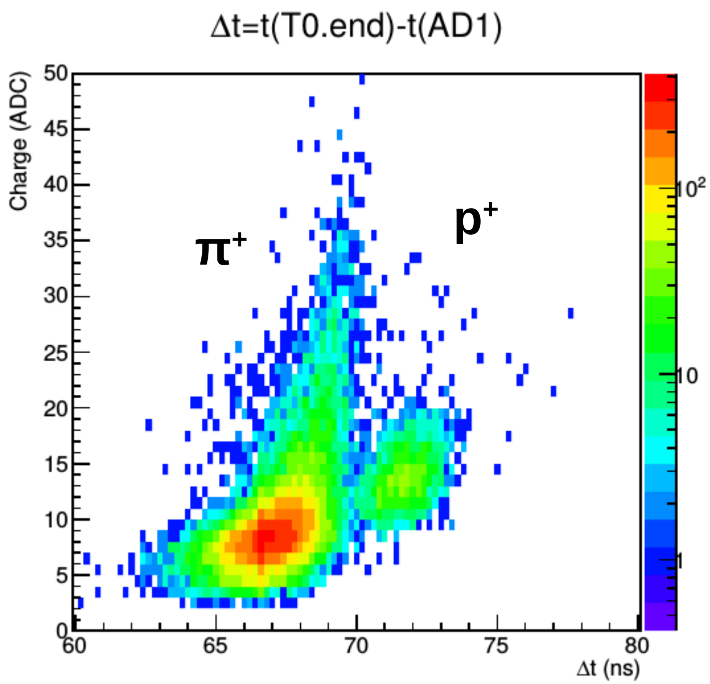

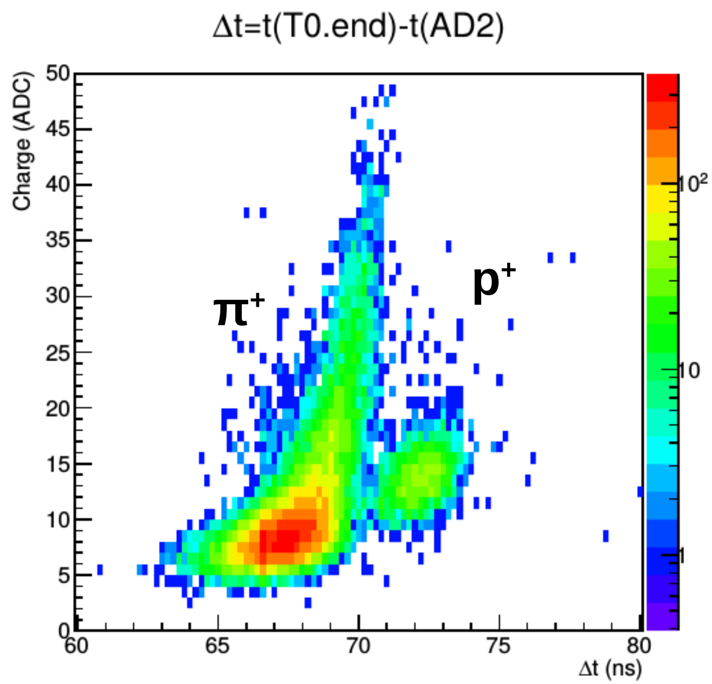

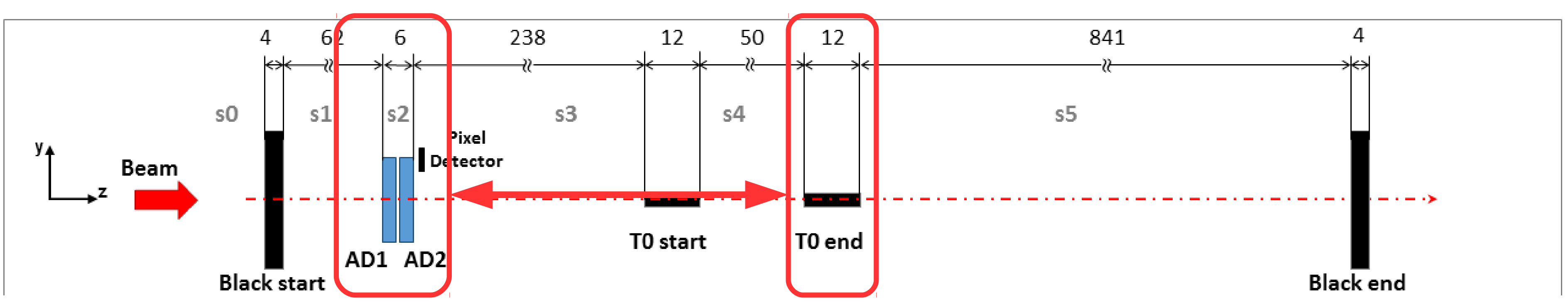

Time measurement

Time slewing

A correction was applied to eliminate the slewing effect due to the pulse amplitude according to:

$$t(Q) = p0 + p1 \cdot Q^{p2}$$

where p0, p1, and p2 are constants parameters.

Once we obtain the parameters from the fit, the time corrected is calculated subtracting the time t(Q) to the measured time:

$$t(\text{corr.}) = t(\text{measured}) - t(Q)$$

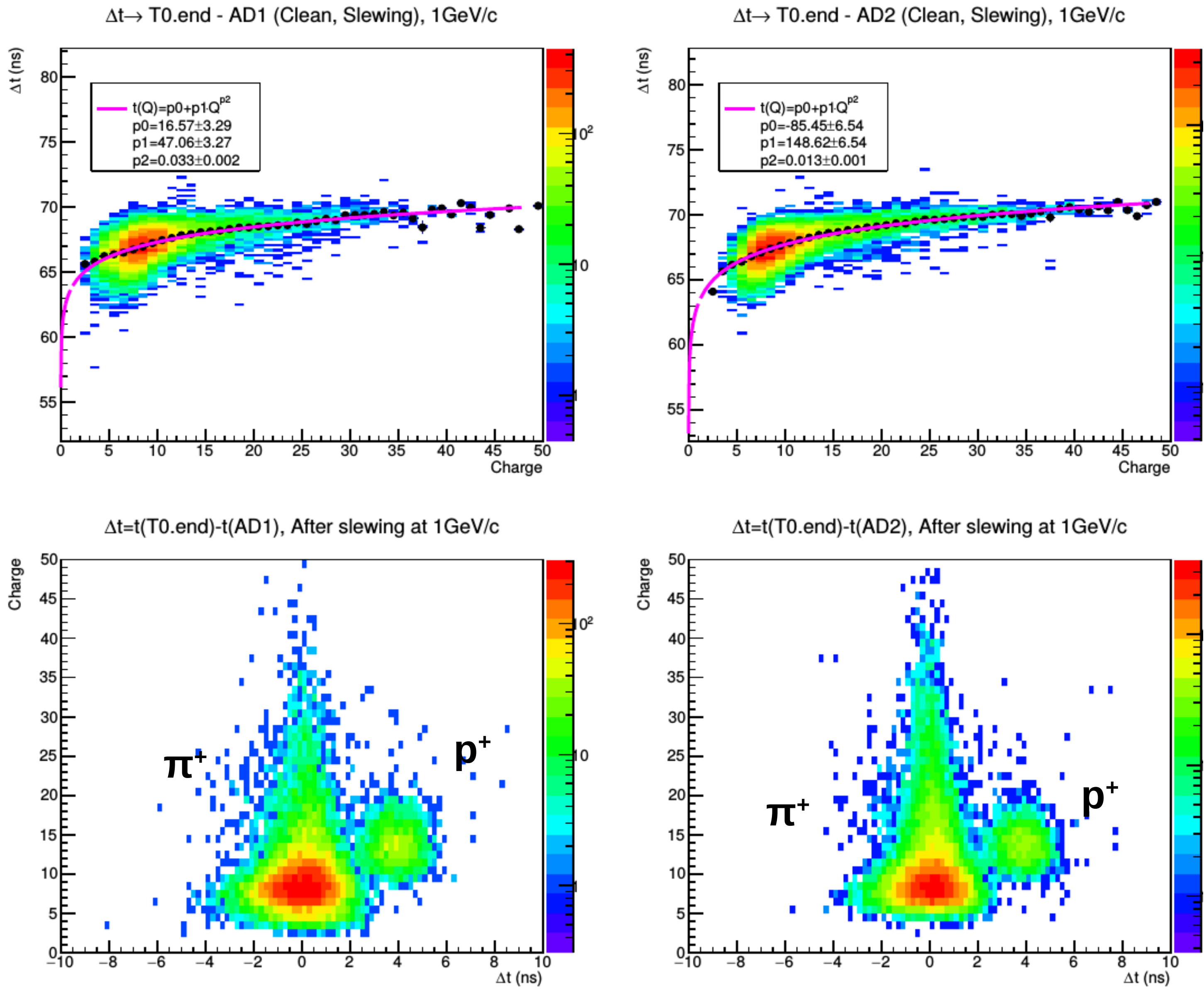

Time measurement

Time slewing

The resolution of the detector after apply the correction (bottom row) have an improvement respect to the one no corrected (top row).

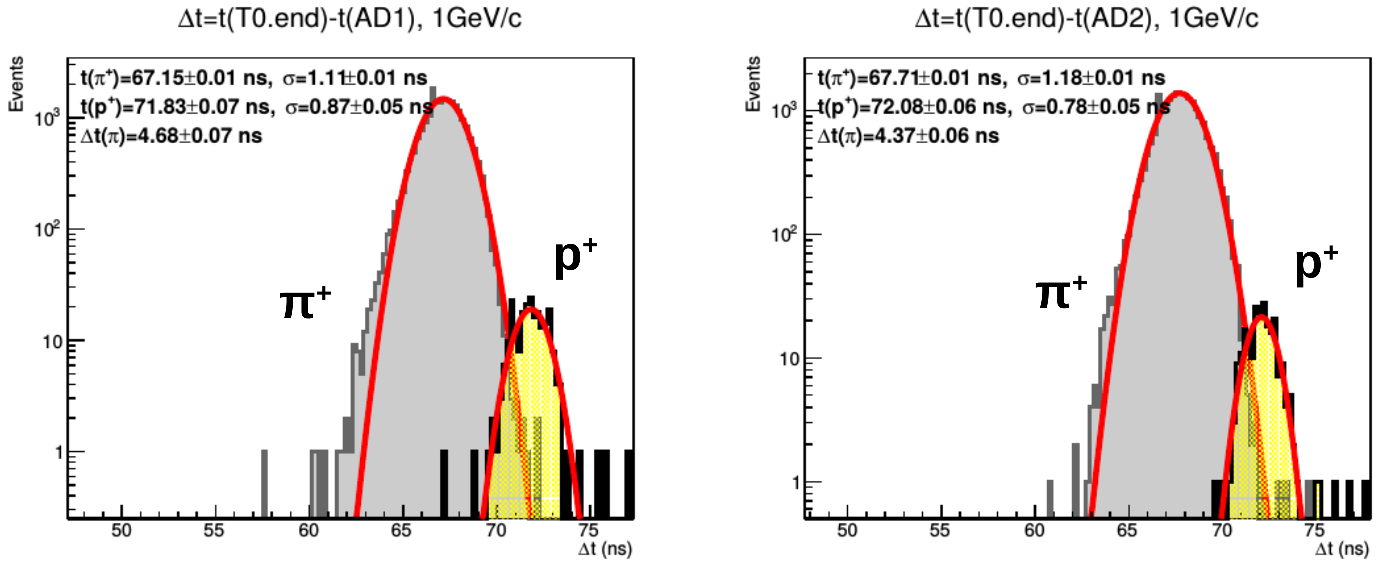

$$t(\text{corr.}) = t(\text{measured}) - t(Q)$$

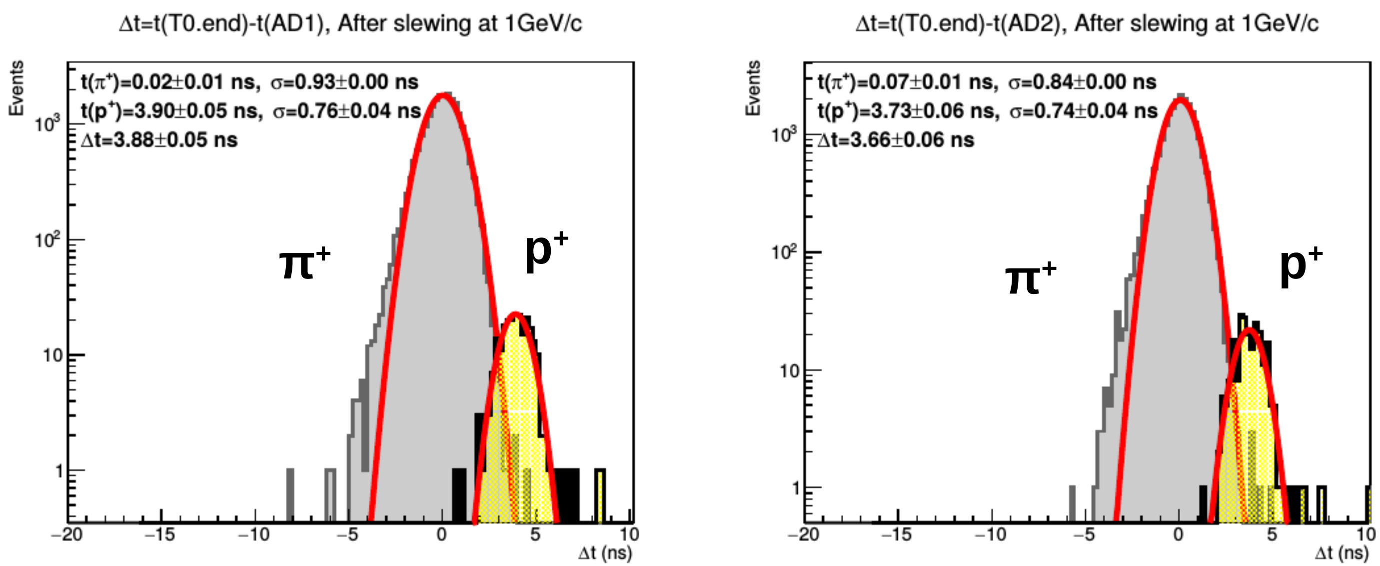

Charge

Charges distributions for 1 GeV/c beam momentum for all particles and pions and protons separated.

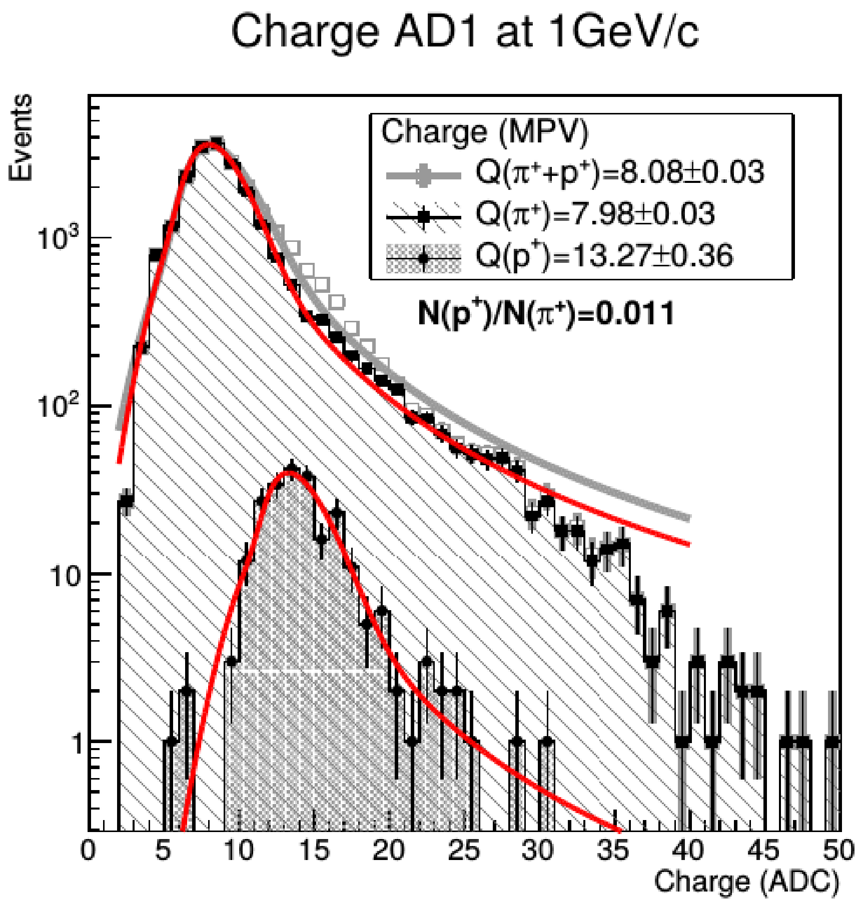

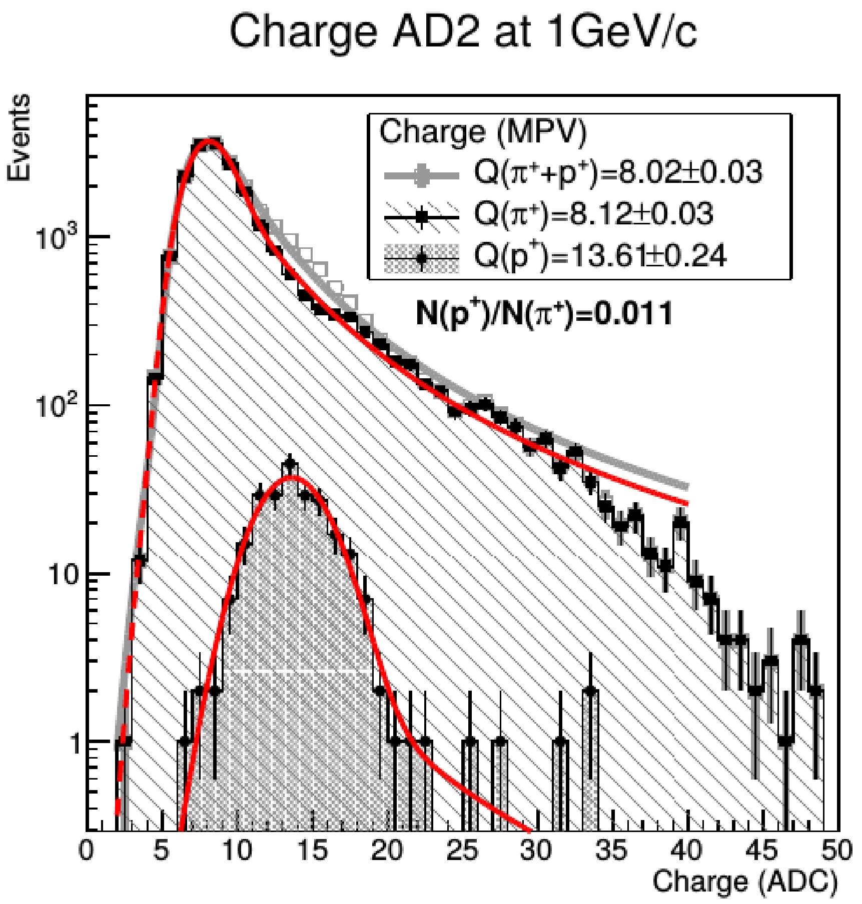

Results

Time - resolution before and after time slewing correction.

Momentum (GeV/c)	AD1 σ (ns)		AD1 Slewing corr. σ (ns)		AD2 σ (ns)		AD2 Slewing corr. σ (ns)	
	π^+	p^+	π^+	p^+	π^+	p^+	π^+	p^+
1.0	1.1 ± 0.01	0.87 ± 0.05	0.93 ± 0.01	0.76 ± 0.04	1.18 ± 0.01	0.78 ± 0.05	0.84 ± 0.01	0.74 ± 0.04
1.5	2.5 ± 0.04	1.43 ± 0.06	1.55 ± 0.02	1.48 ± 0.07	3.11 ± 0.06	1.64 ± 0.07	1.45 ± 0.02	1.54 ± 0.06
2.0	2.6 ± 0.02	1.82 ± 0.03	1.60 ± 0.01	1.7 ± 0.03	3.15 ± 0.03	1.84 ± 0.03	1.44 ± 0.01	1.60 ± 0.02
6.0	1.20 ± 0.03		1.12 ± 0.02		1.27 ± 0.03		1.18 ± 0.02	

Charge – MPV of pions, protons and both combined.

Momentum (GeV/c)	AD1 Charge (ADC counts)			AD2 Charge (ADC counts)		
	$\pi^+ + p^+$	π^+	p^+	$\pi^+ + p^+$	π^+	p^+
1.0	8.08 ± 0.03	7.98 ± 0.03	13.27 ± 0.036	8.02 ± 0.03	8.12 ± 0.03	13.61 ± 0.24
1.5	8.3 ± 0.04	8.18 ± 0.04	9.72 ± 0.16	8.56 ± 0.05	8.45 ± 0.05	9.94 ± 0.13
2.0	8.21 ± 0.02	8.12 ± 0.02	8.80 ± 0.06	8.41 ± 0.02	8.35 ± 0.02	8.89 ± 0.06
6.0	7.23 ± 0.09	-	-	7.14 ± 0.08	-	-

*For the **6 GeV/c** beam momentum was not possible to separate the pions and protons.*

Time measurement
Particle identification

- The composition of the beam in T10 beam facilities is mainly composed by pion and protons.
- Trough Time of flight technique is possible to identify the particles 1, 1.5 and 6 GeV/c.

Theory →
$$\Delta t = t_1 - t_2 = \frac{L}{c}\left[\left(1+\frac{m_1^2c^2}{p_1^2}\right)^{1/2} - \left(1+\frac{m_2^2c^2}{p_2^2}\right)^{1/2}\right]$$

Experiment →
$$\Delta t = t_{AD} - t_{\mathrm{T0-end}}$$

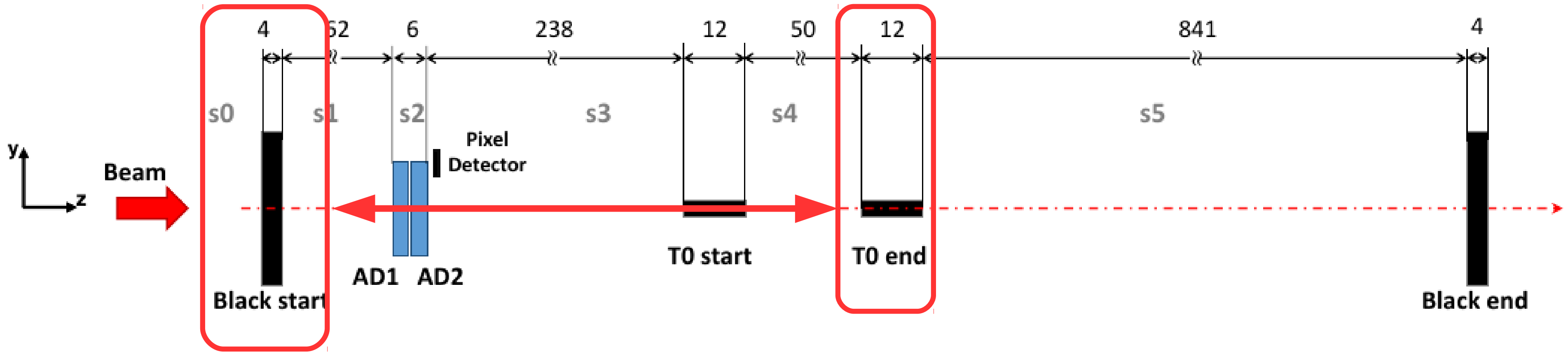

Time measurement

Particle identification (energy deposition)

The particles passing through a detector change its energy because they deposit energy in the material [13]. Such energy is translated to an amount of charge measured, using this we obtained a calibration of the energy deposition in the material. For scintillators detectors the energy loss probability distribution is adequately described by the highly-skewed Landau (or **Landau-Vavilov**) distribution [14].

The most probable energy loss is:

$$\Delta_p = \xi \left(\ln \frac{2mc^2\beta^2\gamma^2}{I} + \ln \frac{\xi}{I} + j + \beta^2 - \Delta(\beta\gamma) \right)$$

donde $j = 0.200$

the density effect correction is negglected $\Delta(\beta\gamma)$

$$\xi = \frac{K}{2}\frac{Z}{A}z^2(x/\beta^2)$$

$$K = 4\pi N_A r_e m_e c^2 = 0.307075 \text{ MeV mol}^{-1} \cdot \text{cm}^2$$

The mean excitation values corresponding to the material were obtained from the experimental measurement (see plot below).

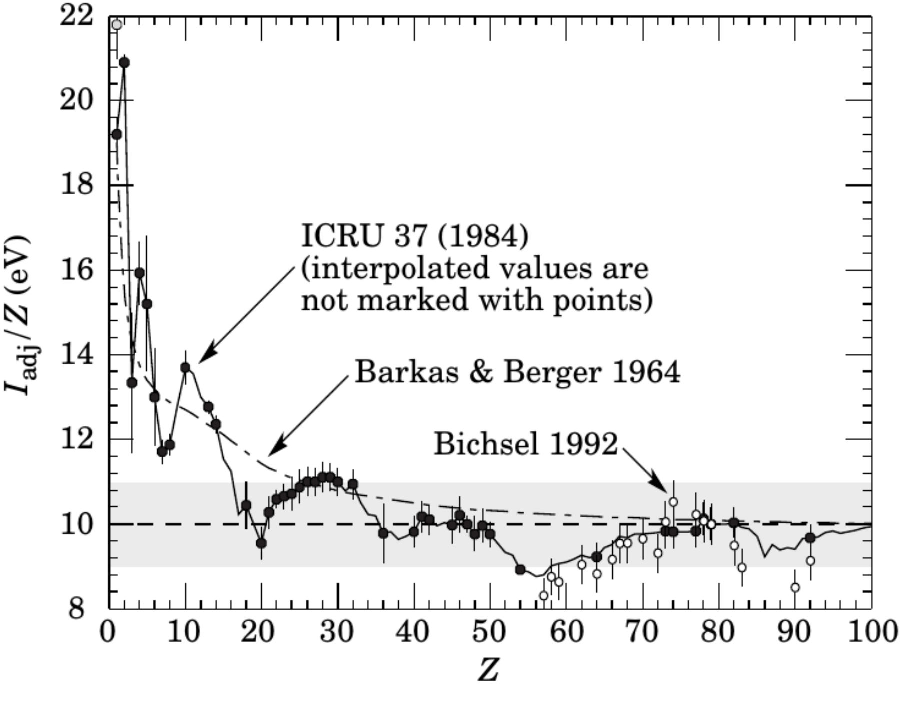

Stages definitions

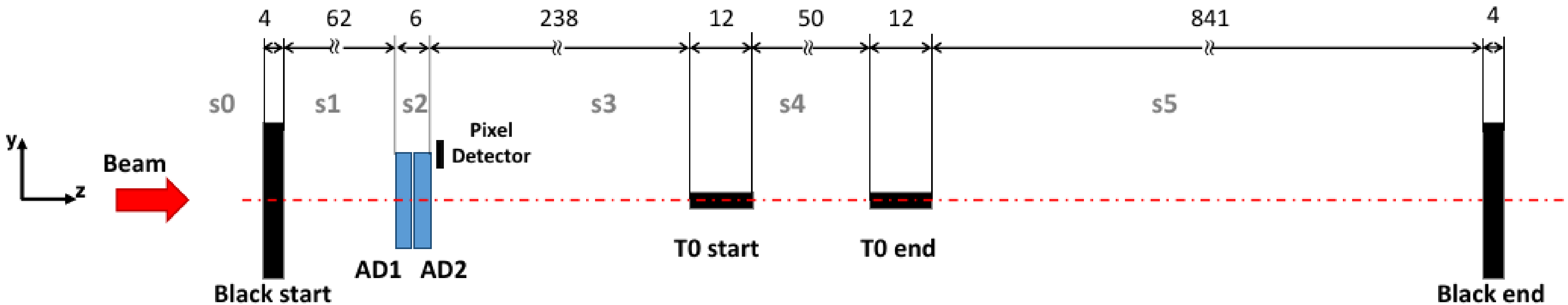

Stage	Placement	Distance (cm)
s0	Before Black-start	-
s1	Black-start to AD1	65.5
s2	AD1 to AD2	3.0
s3	AD2 to T0-start	240.5
s4	T0-start to T0-end	62.0
s5	T0 end to Black-end	854.0

Momentum and energy of the particles before and after interact with the Black-start detector.

Initial momentum (MeV/c)	p_{out} (MeV/c)		E_{in} (MeV)		E_{out} (MeV)	
	π^+	p^+	π^+	p^+	π^+	p^+
1000	988.96	975.63	1009.69	1371.26	998.76	1353.59
1500	1488.75	1484.31	1506.48	1769.28	1495.28	1755.99
2000	1988.54	1986.90	2004.86	2209.15	1993.43	2197.30
6000	5987.56	5988.99	6001.62	6072.92	5989.18	6062.04

Momentum of particles in each stage.

Momentum* (MeV/c)	Pion momentum (MeV/c)					Proton momentum (MeV/c)				
	p_{s1}	p_{s2}	p_{s3}	p_{s4}	p_{s5}	p_{s1}	p_{s2}	p_{s3}	p_{s4}	p_{s5}
1000	988.96	982.21	975.46	964.15	952.84	975.63	960.47	945.10	919.55	892.92
1500	1488.75	1481.87	1474.99	1463.41	1451.85	1484.31	1474.67	1464.99	1449.20	1433.26
2000	1988.54	1981.52	1974.51	1962.52	1950.55	1986.90	1978.88	1970.85	1957.70	1944.52
6000	5987.56	5985.93	5984.30	5977.79	5971.27	5988.99	5982.26	5975.53	5964.31	5953.08

Time of flight difference of the particles in each stage.

$$\Delta t = t_1 - t_2 = \frac{L}{c}\left[\left(1 + \frac{m_1^2 c^2}{p_1^2}\right)^{1/2} - \left(1 + \frac{m_2^2 c^2}{p_2^2}\right)^{1/2}\right]$$

Momentum* (MeV/c)	Time of flight difference (ns/m)					
	Δt_{s0}	Δt_{s1}	Δt_{s2}	Δt_{s3}	Δt_{s4}	Δt_{s5}
1000	1.206	1.229	1.244	1.391	1.463	1.467
1500	0.584	0.593	0.598	0.622	0.635	0.636
2000	0.341	0.338	0.340	0.348	0.352	0.359
6000	0.040	0.040	0.040	0.040	0.040	0.040

The energy loss of the particles leads to an increasing time of flight in each stage after interacting with the material of the detector.

Time of flight

Corrected with the energy deposition

The theoretical time of flight difference between pions and protons of each stage was calculated using the corresponding momentum.

The measured values of the time of flight after and before apply the time slewing correction are compared with the theoretical calculations in the tables below.

1 GeV/c

Detector	Distance (cm)	Theoretical Δt (ns)	Δt (ns)	Slewing corr. Δt (ns)
AD1	305.5	4.067	4.68 ± 0.07	3.9 ± 0.05
AD2	302.5	4.030	4.37 ± 0.06	3.66 ± 0.06
T0.start	62.0	0.907	1.18 ± 0.04	-
Black.start	371.0	4.882	5.27 ± 0.04	4.66 ± 0.03
Black.end	845.0	13.438	14.29 ± 0.09	14.5 ± 0.07

1.5 GeV/c

Detector	Theoretical Δt (ns)	Δt (ns)	Slewing corr. Δt (ns)
AD1	1.809	2.03 ± 0.08	1.83 ± 0.09
AD2	1.791	1.2 ± 0.1	1.68 ± 0.08
T0-start	0.394	0.14 ± 0.01	-
Black-start	2.200	2.1 ± 0.03	2.11 ± 0.02
Black-end	5.824	6.12 ± 0.04	6.29 ± 0.03

2 GeV/c

Detector	Theoretical Δt (ns)	Δt (ns)	Slewing corr. Δt (ns)
AD1	1.010	0.72 ± 0.04	0.66 ± 0.04
AD2	1.000	0.14 ± 0.5	0.54 ± 0.04
T0-start	0.218	1.0 ± 0.01	-
Black-start	1.233	1.19 ± 0.02	1.09 ± 0.02
Black-end	3.288	3.21 ± 0.09	3.77 ± 0.01

Energy calibration

Theoretical energy deposition in AD1 and AD2.

Momentum* (MeV/c)	AD1 (MeV)		AD2 (MeV)		Energy ratio (p^+/π^+)	
	π^+	p^+	π^+	p^+	AD1	AD2
1000	6.685	10.885	6.683	10.954	1.628	1.639
1500	6.853	8.138	6.850	8.157	1.188	1.191
2000	7.000	7.248	6.998	7.255	1.035	1.037
6000	7.632	6.652	7.632	6.651	0.872	0.872

Energy calibration in AD1 and AD2:

ration of the energy deposited and the charge measured in each detector.

Momentum* (MeV/c)	AD1 (MeV/ADC)		AD2 (MeV/ADC)	
	π^+	p^+	π^+	p^+
1000	0.8377 ± 0.0031	0.8203 ± 0.0022	0.8230 ± 0.0030	0.8049 ± 0.0142
1500	0.8377 ± 0.0041	0.8372 ± 0.0138	0.8107 ± 0.0048	0.8206 ± 0.0107
2000	0.8620 ± 0.0021	0.8236 ± 0.0056	0.8380 ± 0.0020	0.8161 ± 0.0055

The energy deposited calculated respect to the measured charge are consistent.
The average value of the calibration is:

$$\varepsilon = 0.8322 \pm 0.0124 \text{ MeV/ADC}$$

Other sections
Charge, time and efficiency

Charge and efficiencies of the different sections of the detector.

Section	AD1 Charge (ADC counts)	AD2 Charge (ADC counts)	AD1 Efficiency (%)	AD2 Efficiency (%)
Border	8.42 ± 0.02	9.24 ± 0.01	78.94 ± 0.09	71.6 ± 0.08
Conn. 1	1.31 ± 0.56	0.34 ± 0.21	2.78 ± 0.53	4.85 ± 0.7
Conn. 2	6.27 ± 1.38	0.27 ± 0.18	8.24 ± 0.91	7.81 ± 0.88
Fibres	3.66 ± 0.14	2.14 ± 0.02	10.99 ± 0.15	8.66 ± 0.14
PMT	3.59 ± 0.39	2.56 ± 0.001	38.94 ± 1.06	40.25 ± 1.07

Time resolution after the time slewing correction.
Time difference of the signal generated in each section with respect to the center of the AD module.

Section	AD1: σ (ns)		AD2: σ (ns)		AD1 (ns)	AD2 (ns)
	π^+	p^+	π^+	p^+	Δt (w.r.t. center)	
Center	7.98 ± 0.03	13.27 ± 0.036	8.12 ± 0.03	13.61 ± 0.24	0 ± 0.01	0 ± 0.01
Border	0.89 ± 0.01	0.83 ± 0.02	0.81 ± 0.001	0.85 ± 0.03	0.19 ± 0.03	0.6 ± 0.01
Conn. 1	1.17 ± 0.2	0.95 ± 0.3	1.54 ± 0.26	0.43 ± 0.14	-0.27 ± 0.92	0.55 ± 0.32
Conn. 2	0.75 ± 0.7	0.37 ± 0.13	1.27 ± 0.12	0.56 ± 0.2	-0.1 ± 0.44	0.82 ± 0.15
Fibres	0.81 ± 0.02	-	0.99 ± 0.3	-	7.97 ± 0.01	7.25 ± 0.05
PMT	0.68 ± 0.03	-	0.89 ± 0.05	-	8.47 ± 0.01	7.77 ± 0.07

Time Resolution

The comparison of the global time resolution, see Table 8.5, and what is reported in [45] (300 and 500 ps in ADA and ADC respectively) do not match; nevertheless the dependency of the time resolution with respect to the charge have been considered.

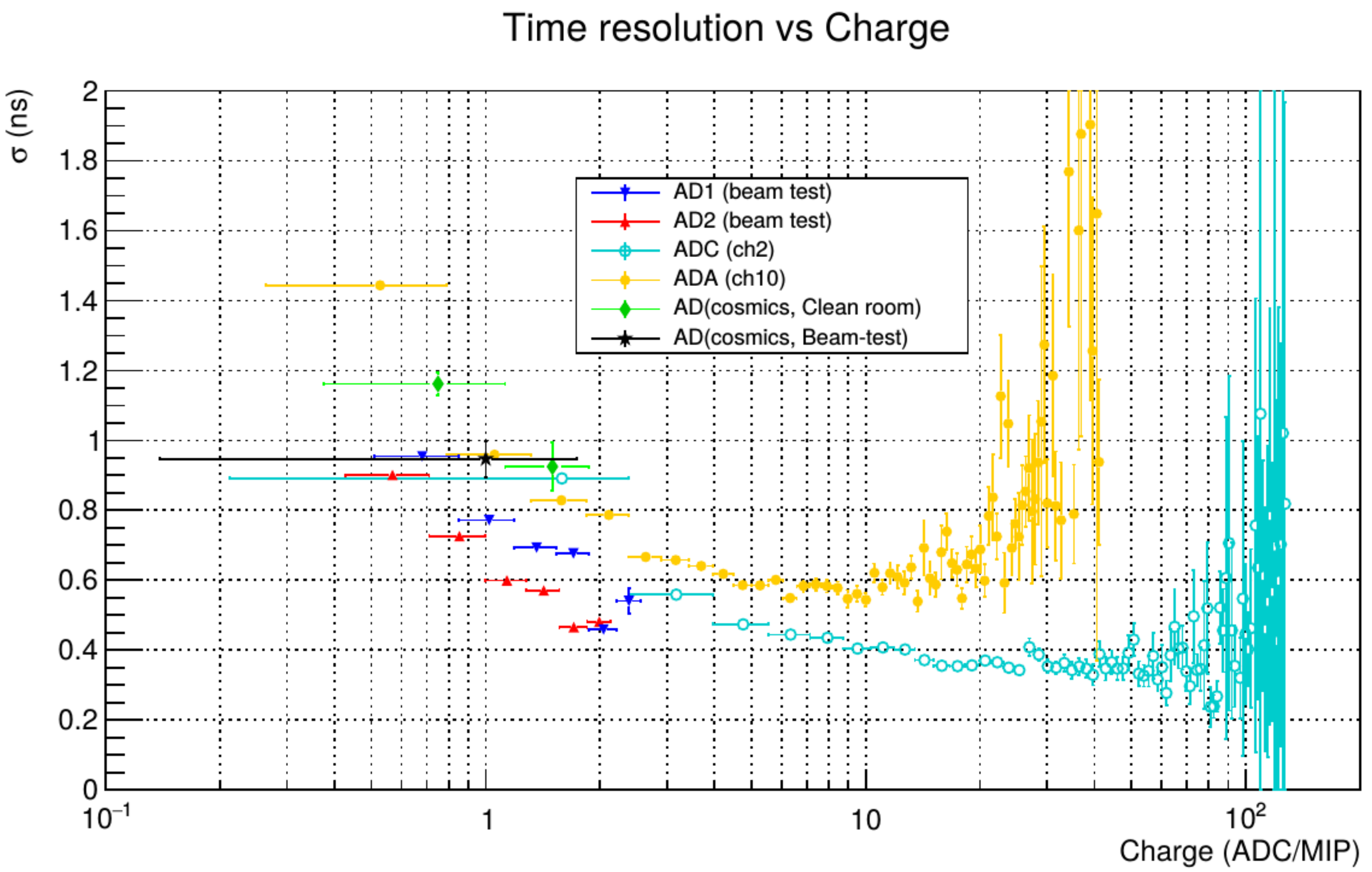

Final comments.

- The results have been included in the Monte Carlo analysis.
- Technical note of the Beam test performance. Work in progress.
- Is an important reference for the AD upgrade (Forward Diffractive Detector) for the Run II.

Thank you!

Bibliography

1) Measurement of inelastic, single- and double-diffraction cross sections in proton-proton collisions at the LHC with ALICE, The ALICE Collaboration, Junio 8, 2013. *Eur.Phys.J.*
2) A Study of Diffractive Production in ALICE, O. Villalobos Baillie, 2012. *Journal of Physics.*
3) Diffractive Physics, A.D. Martin, H. Hoeth, et. al., Junio 12, 2012. *PoS QNP2012 (2012) 017*
4) Diffractive physics in ALICE at the LHC, Gerardo Herrera Corral. *AIP Conf. Proc*.
5) Diffraction physics with ALICE at the LHC, Sergey Evdokimov, Diciembre 24, 2014. *Conference C14-06-23.7.*
6) Diffraction and rapidity gap measurements with the ATLAS detector, Pauline Bernat, Octubre 20, 2012. *ATL-PHYS-PROC 2012-233, ATL.PHYS-PROC-2012-1275.*
7) Report of the Working Group on Diffractive Physics and Color Coherence, Michael Albrow, Andrew Brandt, Alfred Mueller, Carl Schmidt. *Inspire 541307.*
8) New Forward and Diffractive Physics at CMS, Alberto Santoro, 2011. *J. Phys.*
9) Pomeron Physics and QCD, O. Nachtmann, Diciembre 19, 2003. *HD-THEP-03-63*
10) O. V. Baillie, the Alice Collaboration, A study of diffractive production in 124 ALICE, Journal of Physics: Conference Series 381 (1) (2012) 012039.
11) S. Evdokimov, Difraction physics with ALICE at the LHCarXiv:1412.127.7300.
12) Front end electronics and first results of the ALICE V0 detector, Y. Zoccarato et. al., 6 October 2010, Nuclear Instruments and Methods in Physics Research A.
13) C. Grupen, B. Schwartz, Particle Detectors, second edition Edition, Cambridge monographs on particle physics and cosmology., 2008.
14) N. Radiation Physics Division, PML, Tables of x-ray mass attenuation coefficients and mass energy-absorption coefficients from 1 kev to 20 mev for elements z = 1 to 92 and 48 additional substances of dosimetric interest (July 2004).

Appendix

FEE connexion

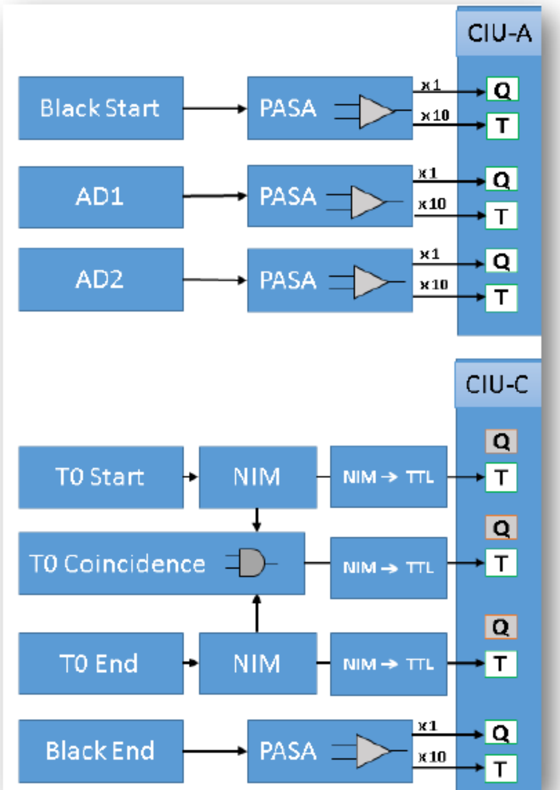

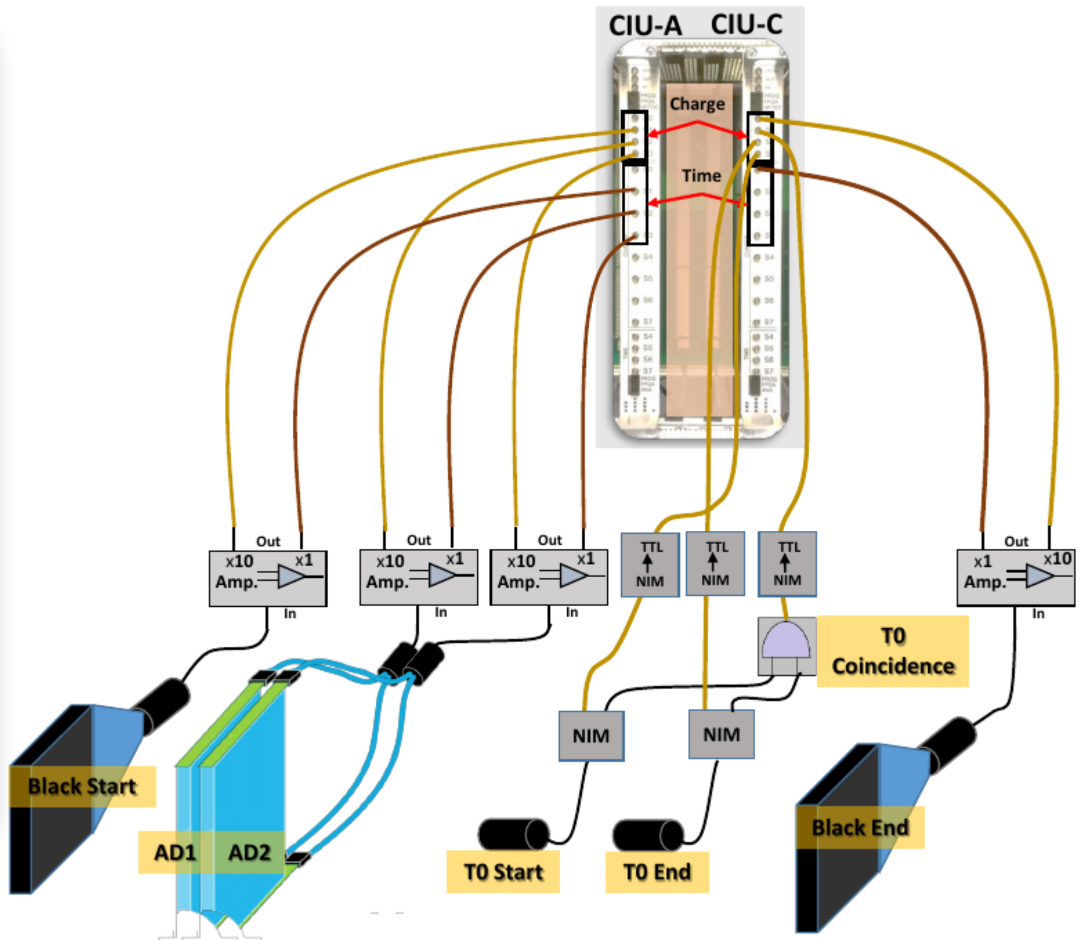

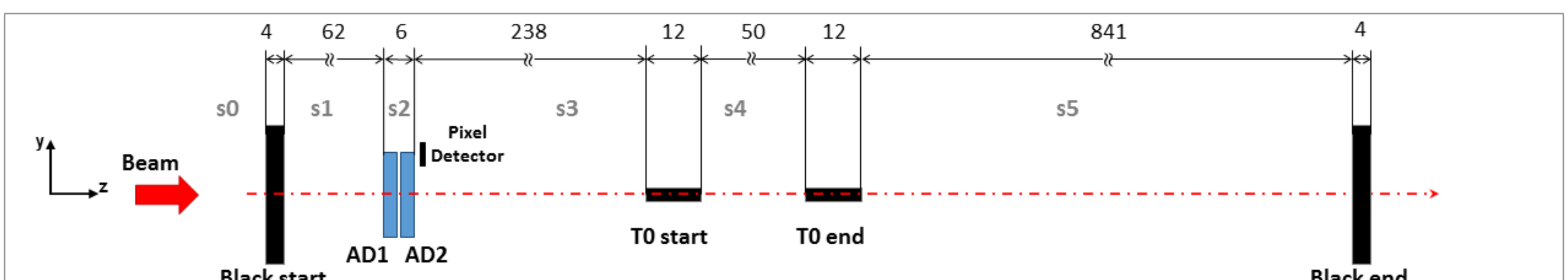

Air gap identification

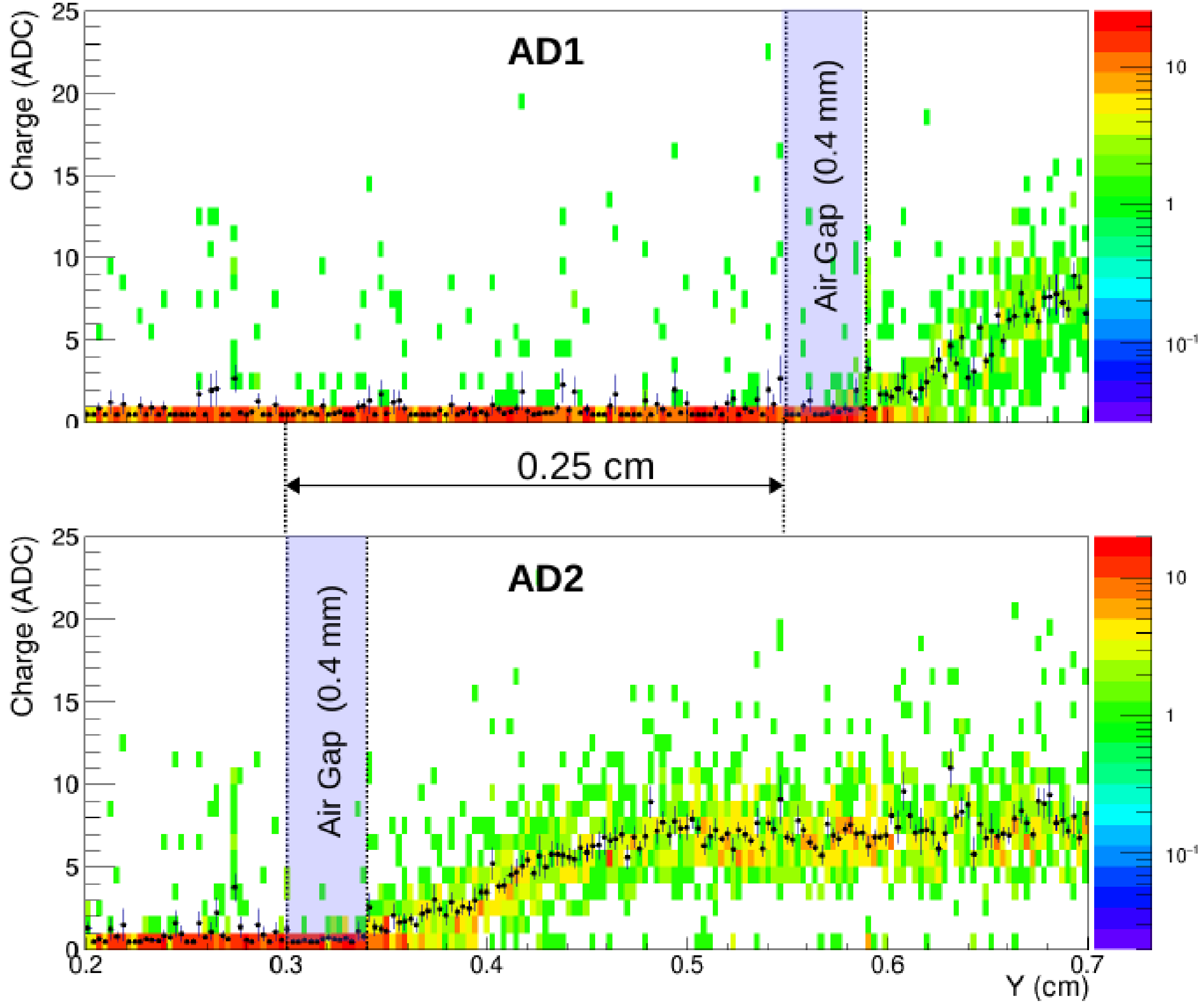

AD1 → Charge vs Y (pixel position)

Selection of event in WLS Bar and plastic scintillator

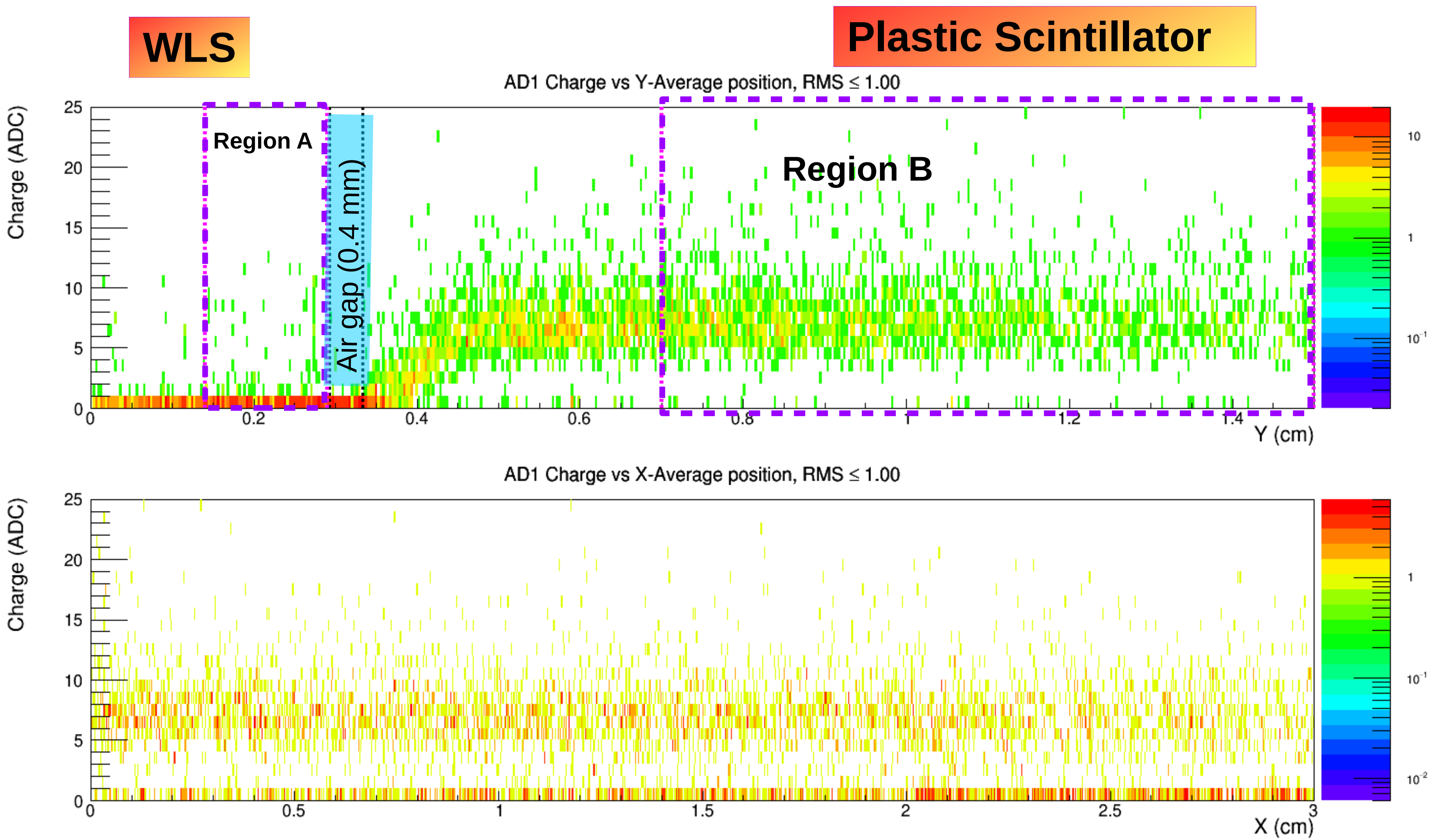

Top plot: Region **A** and **B** defined on **AD1** module along the **Y axis**.
Bottom plot: The **charge** along the **X axis** looks homogeneous.

AD2 → Charge vs Y (pixel position)

Selection of event in WLS Bar and plastic scintillator

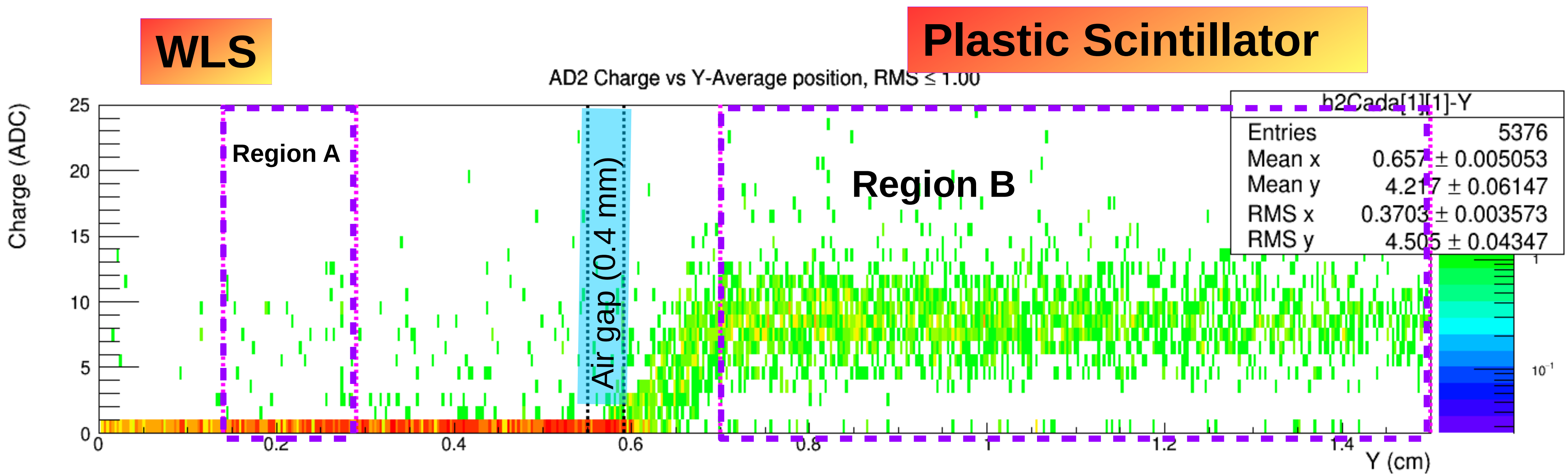

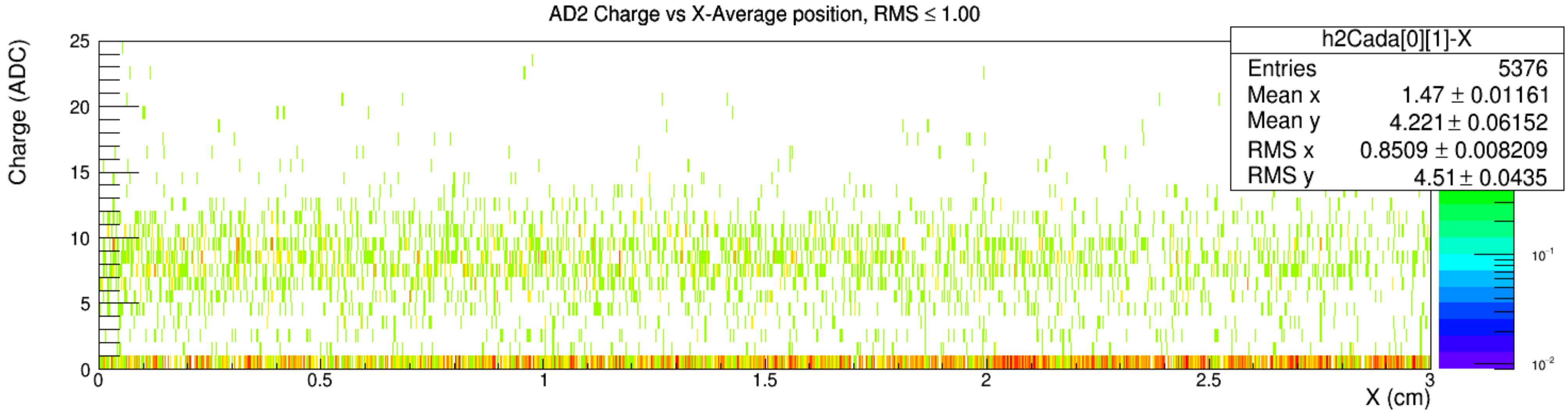

Top plot: Region **A** and **B** defined on **AD2** module along the **Y axis**.
Bottom plot: The **charge** along the **X axis** looks homogeneous.

RMS cleaning

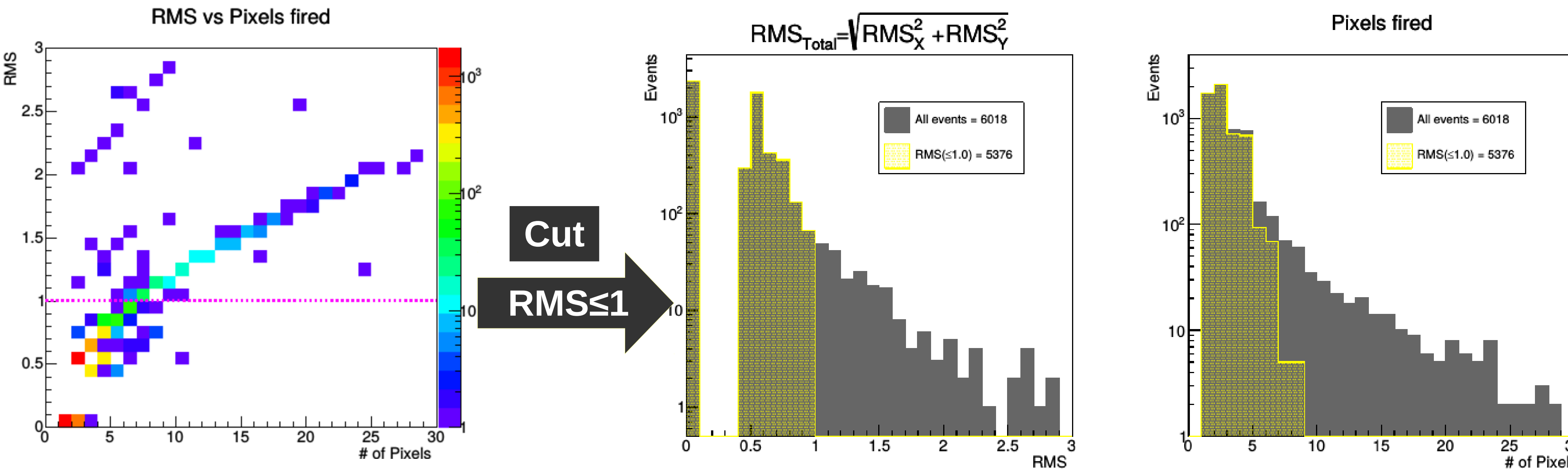

$$\mathrm{RMS} = \sqrt{\mathrm{RMS}_X^2 + \mathrm{RMS}_Y^2}$$

$$\mathrm{RMS}_X = \sqrt{\frac{1}{N}\sum_i (x_i^2 - x_{\mathrm{mean}}^2)} \qquad \text{and} \qquad \mathrm{RMS}_Y = \sqrt{\frac{1}{N}\sum_i (y_i^2 - y_{\mathrm{mean}}^2)}$$

Energy deposition

The particles passing through a detector change its energy because they deposit energy in the material [81]. Such energy is translated to an amount of charge measured, using this we obtained a calibration of the energy deposition in the material. For scintillators detectors the energy loss probability distribution is adequately described by the highly-skewed Landau (or Landau-Vavilov) distribution [82].

The most probable energy loss is:

$$\Delta_p = \xi\left(\ln\frac{2mc^2\beta^2\gamma^2}{I} + \ln\frac{\xi}{I} + j + \beta^2 - \Delta(\beta\gamma)\right) \qquad \xi = \frac{K}{2}\frac{Z}{A}z^2(x/\beta^2)$$

m = mass of the particle (eV/c²).
c = speed of ligth.
β = pc/E.
E = energy of the particle (eV).
βγ=p/mc.
j = 0.2
I = mean exitation value (eV).
Δ(βγ)= density effect correction.

K = $4\pi N A\, r_e\, m_e\, c^2$ = 0.307075 MeV mol^{-1}· cm²
Z = atomic number
A = atomic mass
z = charge
x = detector thickness (g/cm²)

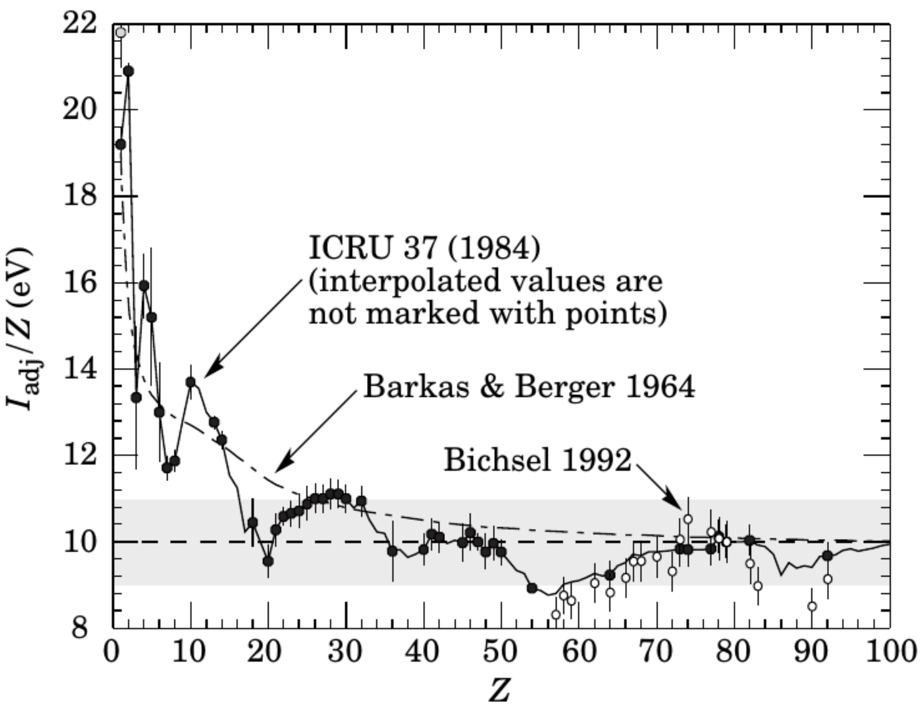

Resolución temporal

Se seleccionó la distribución de carga para analizar la resolución temporal a diferentes cargas.

Selección de cargas con datos de la prueba de haz (AD1).

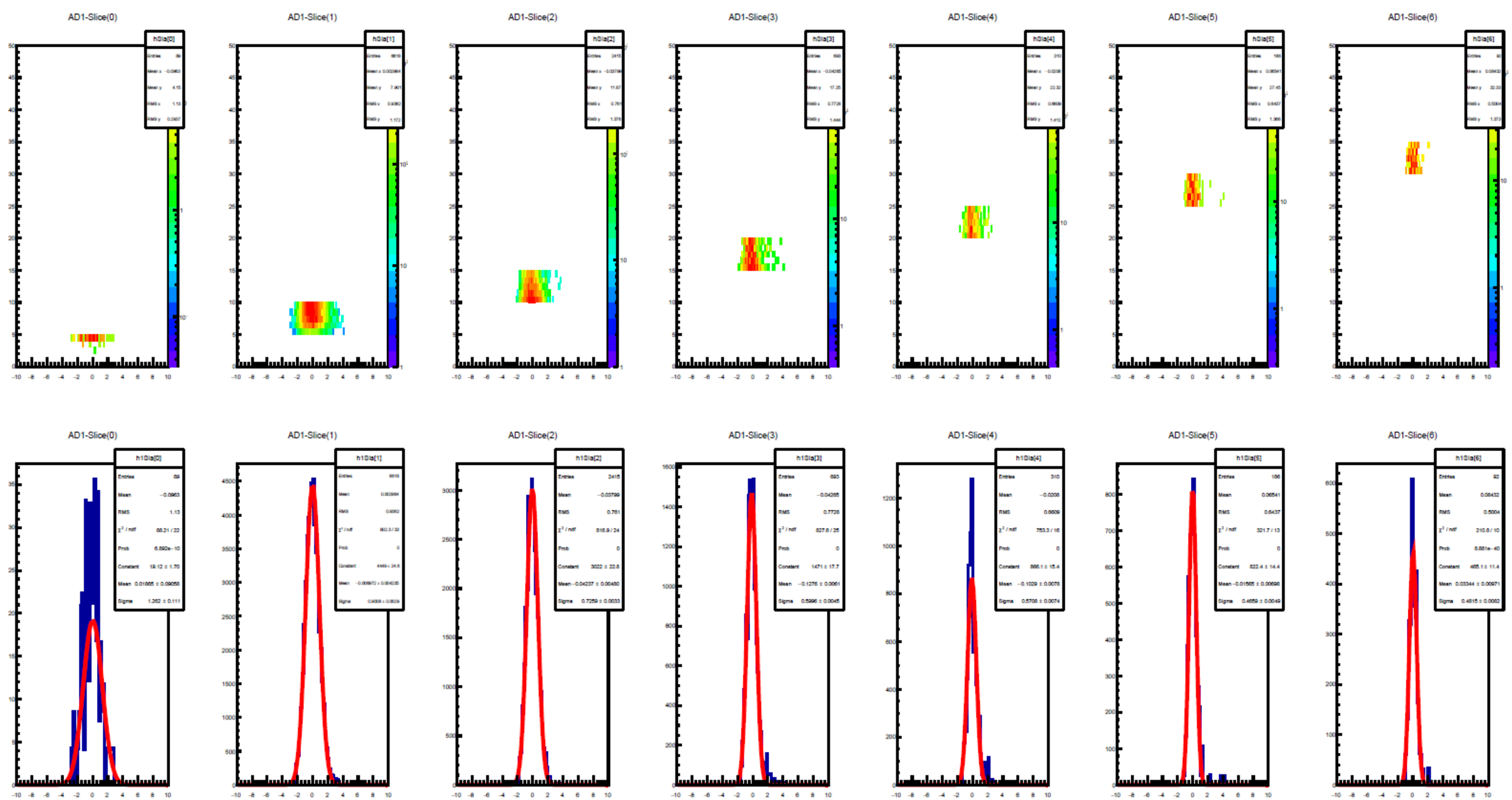

Beam test

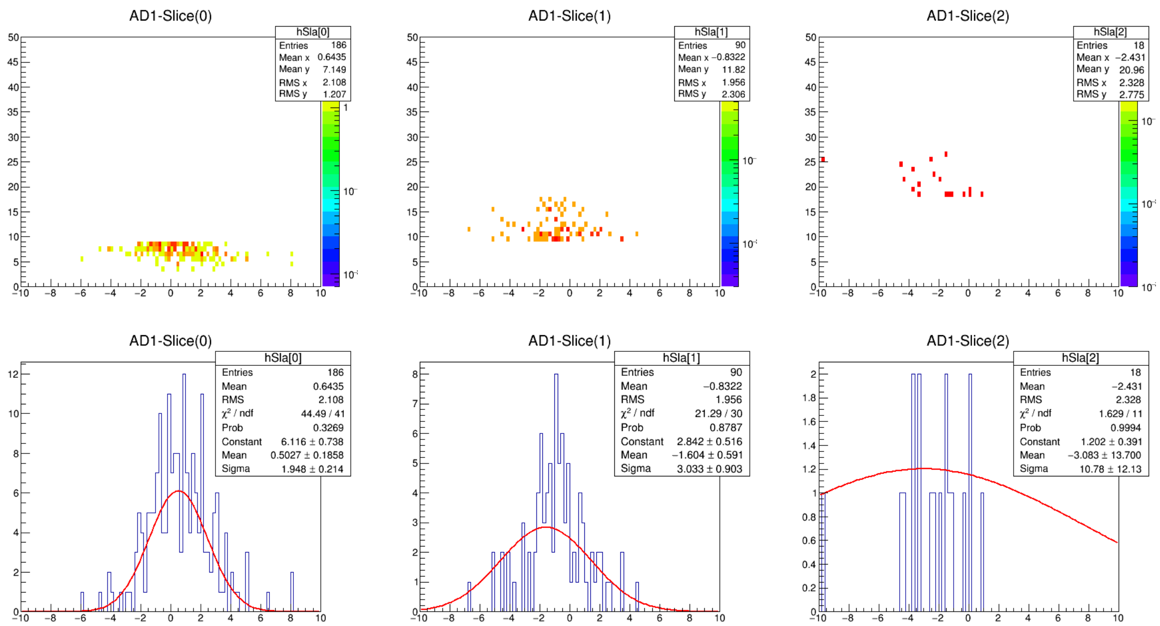

Clean room

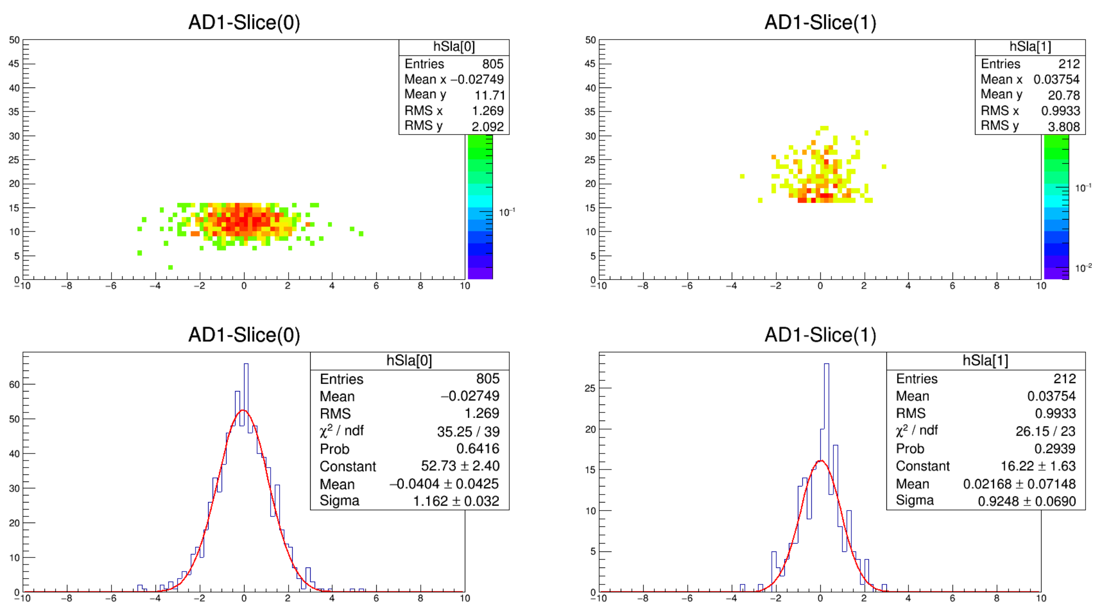

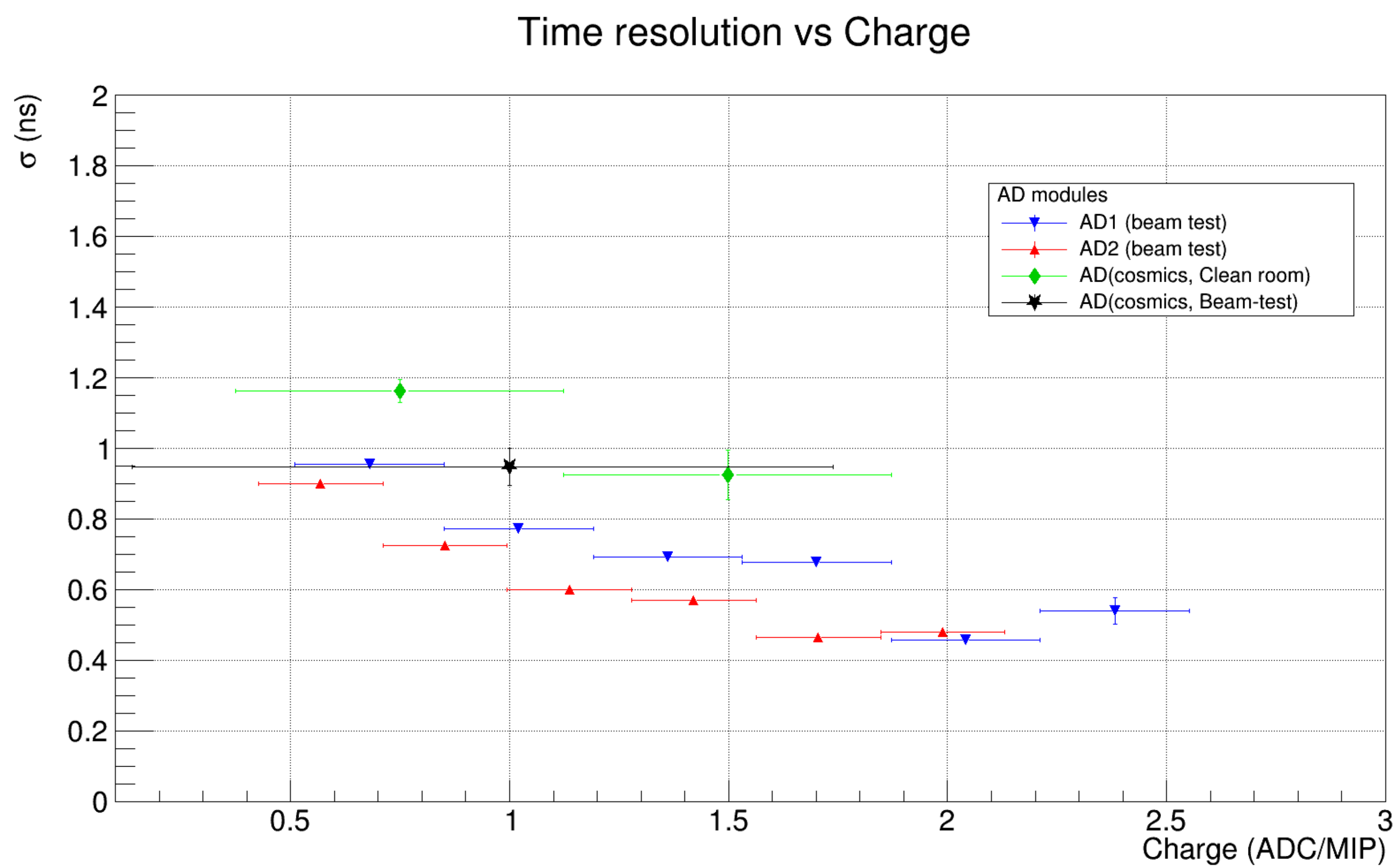

Time resolution vs Charge
σ (ns)
Charge (ADC/MIP)
AD modules
AD1 (beam test)
AD2 (beam test)
AD(cosmics, Clean room)
AD(cosmics, Beam-test)
0
0.2
0.4
0.6
0.8
1
1.2
1.4
1.6
1.8
2
0.5
1
1.5
2
2.5
3

Resolución temporal

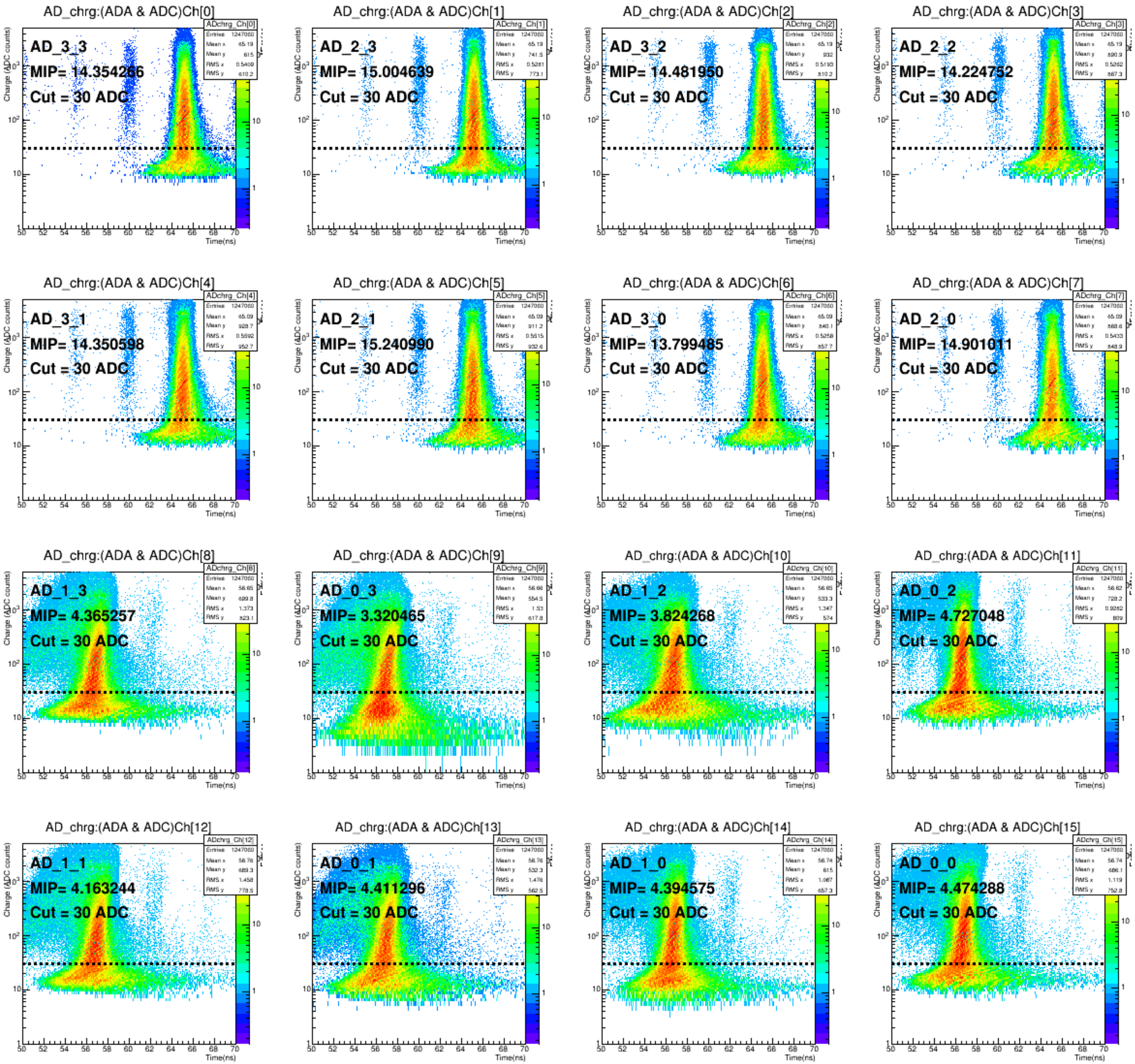

ADC

ADA

Results using pixel detector

Charges (ADC counts)

	WLS (mean)
AD1	0.34 ± 0.06
AD2	0.10 ± 0.03
AD	**0.22 ± 0.08**

Efficiency (%)

	WLS
AD1	3.69 ± 0.67
AD2	3.26 ± 0.32
AD	**3.47 ± 0.74**